April 2015
Volume 121
Issue 1948
£5.20

www.electronicsworld.co.uk

Electronics WORLD

THE ESSENTIAL ELECTRONICS ENGINEERING MAGAZINE

Special report:
Design with sensors and networks to support them

INTRODUCING FTDI CHIP'S SUPERSPEED USB 3.0 SOLUTION

SUPERSPEED CERTIFIED USB

ALSO IN THIS ISSUE:

- Software Defined Radio
- UWB LNA Design
- Raspberry Pi Projects

@FTDIChip
www.ftdichip.com

Technology
Industry and academia tackle student crisis

Feature Series:
RF design

Products
Latest T&M equipment and systems

*A shipping charge of £12.00 will be billed on all orders of less than £50.00. All orders are shipped via UPS for delivery within 1-3 days (dependent on final destination). No handling fees. All prices are in British pound sterling and include duties. If excessive weight or unique circumstances require deviation from this charge, customers will be contacted prior to shipping order. Digi-Key is an authorized distributor for all supplier partners. New product added daily.

Cover supplied by FDTI CHIP
More on pages 18-19

REGULARS

FEATURES

Free Your Creativity

with Core Independent Peripherals

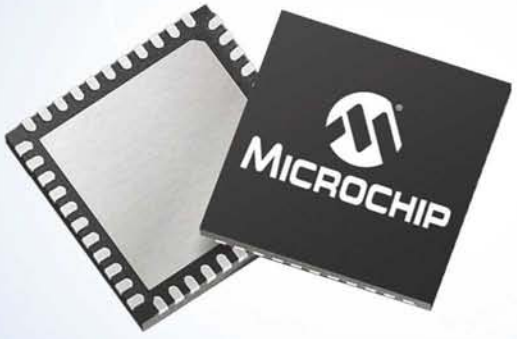

FLEXIBLE INTELLIGENCE MADE EASY

8-BIT PIC® MICROCONTROLLERS

PIC® microcontrollers with Core Independent Peripherals take 8-bit MCU performance to a new level. With a number of on-board modules designed to increase capability in any control system, these MCUs represent the best value in embedded design.

Core Independent Peripherals are designed to handle their tasks with no code or intervention from the CPU to maintain operation. As a result, they both simplify the implementation and boost the performance of complex control systems while giving designers the flexibility to innovate.

Flexible Functional Building Blocks

- Power conversion
- Motor drive
- Signal generation
- Sensor interface

microchip DIRECT
www.microchipdirect.com

MICROCHIP

www.microchip.com/get/eucip

THE CHALLENGE OF PROTECTING INNOVATIONS IN MEDICAL ELECTRONICS

Telehealth systems are aimed at home care and/or remote monitoring and, as such, are increasingly drawing the attention of medical technology developers; however, they can present unique intellectual property (IP) issues.

Telehealth developments are often based on new software, particularly for user interfaces, data processing methods and communications protocols. Patenting software can be very difficult, especially in Europe. Furthermore, the main user is often the patient, in their own home. Such "private" use is not considered patent infringement in many jurisdictions. Obtaining effective patent protection for telehealth innovations can therefore be challenging.

Patent law differs between countries, but if a software invention can be patented in Europe then it should be patentable in most jurisdictions. The US patent office in particular has historically been far more ready to grant patents for computer-based inventions than its European counterpart (although it has become less permissive in recent years). The following is based on the current situation in Europe, but many points will apply worldwide.

Take, for example, a telehealth system comprising a monitoring device that transmits measurement data to a patient's computer, software on the computer which collates the data and transmits it to a medical facility, and a computer at a medical facility which receives the measurement data. Certain aspects of this system are potentially patentable (provided they are new), whilst others are not.

First it should be asked if the aspects that are new and innovative are technical aspects. Consider, for instance, an algorithm for automatically classifying received measurements, included in the patient-end software. If this algorithm merely automates what a nurse would do, for example label each measurement with a date, time and patient ID, this aspect of the system would not be sufficiently technical to be the subject of a patent. If, however, a "further technical effect" stems from the classification, patent protection could well be possible. For example, an algorithm configured to compare each measurement to predetermined criteria and thereby generate a score of the patient's disease risk is likely to be deemed sufficiently technical for a patent.

If patent protection seems advisable for a particular aspect, then various other legal considerations come into play. In Europe and the UK, for instance, rules prevent the patenting of treatment methods for the human body and diagnostic methods practised on the human body. These exclusions are likely to be relevant to telehealth systems that automatically generate a diagnosis and/or administer a treatment. Diagnostic methods are only excluded if the patent claim includes all the steps necessary to reach a medical decision on diagnosis and if all the technical steps of the method require the presence of the patient. The treatment method exclusion is broader and effectively prevents the patenting of any method involving treating the body – even if it's just one step. The exclusions do not apply to the apparatus that performs the method, but they can be a barrier to obtaining patent protection in cases where an existing apparatus is put to new use, or where the apparatus is just an obvious combination of known devices.

> The IP challenges presented by telehealth systems are generally not insurmountable, but obtaining the strongest possible protection for a new innovation requires careful consideration

A further important consideration is the feasibility of enforcing the resulting patent. If your patent is directed to a particular algorithm run by the controller of a medical monitoring device, could you detect that a competitor's device was using the same algorithm? In such cases it is often possible to design the algorithm and/or device to make such detection possible, and it is therefore a good idea to consider detectability during the design and development of telehealth systems. If the nature of the innovation means detection will always be difficult or even impossible, then it is advisable to consider if there is any benefit in obtaining patent protection for that particular innovation.

A related question is who the potential infringer may be. There may not be much value in patenting a method that will only ever be performed by a patient, and this could easily be the case for many processes associated with telehealth systems. If patent protection for the apparatus itself can't be obtained, then ideally a patent should be directed to a method that must be performed by the manufacturer or a commercial operator of the telehealth system, e.g. during installation or testing of the system.

So, the IP challenges presented by telehealth systems are generally not insurmountable, but obtaining the strongest possible protection for a new telehealth innovation requires careful consideration, both during the design and development of the product and also in crafting patent application(s) to cover it.

Michelle Claydon, UK and European Patent Attorney at European intellectual property practice Haseltine Lake, discusses the challenges of obtaining and enforcing IP protection for telehealth, home care and remote medical monitoring systems

EDITOR: Svetlana Josifovska
Tel: +44 (0)1732 883392
Email: svetlanaj@sjpbusinessmedia.com

SALES: Sunny Nehru
Tel: +44 (0)20 7933 8974
Email: sunnyn@sjpbusinessmedia.com

DESIGN: Tania King
PUBLISHER: Justyn Gidley

ISSN: 1365-4675

PRINTER: Buxton Press Ltd

SUBSCRIPTIONS:
Subscription rates:
1 year: £62 (UK);
£89 (worldwide)
Tel/Fax +44 (0)1635 879361/868594
Email: electronicsworld@circdata.com

SJP business media
2nd Floor,
52-54 Gracechurch Street,
London, EC3A 0EH

Follow us on Twitter
@electrowo

Join us on LinkedIn

TECHNOLOGY FIRMS PARTNER WITH UNIVERSITIES TO TACKLE STUDENT CRISIS

Technology companies are focusing on attracting more students to engineering courses

Top technology companies are increasingly getting involved in university courses to help attract more students to engineering disciplines and shape the next generation of engineers.

Microprocessor IP firm ARM announced its partnership with UCL (University College London) over a new Internet of Things (IoT) education kit. The aim is to encourage more graduates to stay in Science, Technology, Engineering and Maths (STEM) professions, since statistics suggest that half leave the sector to pursue careers in unrelated areas.

"Students with strong science and mathematical skills are in demand, and we need to make sure they stay in engineering," said Mike Muller, ARM's chief technology officer. "New technologies make it far easier to start a business, and there's a huge appetite for highly-motivated young people to help companies such as ARM deliver innovation that will shape the world's future."

Latest research carried out by UCL showed that of those in engineering 36% male and 51% female graduates took up non-STEM careers; the numbers are 44% male and 53% female for those in technology.

"Many students are not following through to an engineering career and that is a real risk to our long-term success as a nation of innovators," said Professor Izzat Darwazeh, head of communications and information systems at UCL Engineering Sciences. "Students take engineering because they are driven to understand how the world works, from taking radios apart when they were children, to creating apps in high school. Engineering is about creative problem-solving and it's exactly what we hope to instil in them and provide the tools and knowledge to create devices and systems that could one day become best sellers or even change our world."

UCL is also trying to attract more women into engineering with free masters degrees, fully-funded bursaries and fee waivers. The University says that only 7% of the engineering workforce in the UK is female, lower than any other country in Europe.

"We want to encourage more women to apply as they are currently vastly under-represented in engineering. The Scheme offers mentoring by researchers and senior managers from technology companies to provide a fantastic boost to what can be a wonderful career for a woman to pursue," said Jane Butler, Vice Dean at UCL Engineering.

Elsewhere, the Universities of Leeds and Sheffield partnered with UKESF (UK Electronics Skills Foundation) to increase uptake of electronics degrees in general. They join 11 other universities as part of a programme to address the overall decline in the number of British students applying and registering for Electrical and Electronic Engineering degrees.

"By working with more of the UK's leading universities, we are able to introduce our industry partners to a wider pool of the most talented electronic engineering students for sponsorship through university. And by providing work experience placements for them, our sponsors are able to develop relationships as an early start to their graduate recruitment process," said Indro Mukerjee, chairman of the UKESF strategic advisory board.

Through its scholarship scheme, UKESF helps students find work placements with about 25 industry sponsors, including its industry founders and partners ARM, AWE, CSR, Dialog Semiconductor, Imagination Technologies, Thales and XMOS.

It is anticipated that by 2020 the UK electronics industry may be worth £120bn and generate 150,000 highly skilled jobs; however, UCAS data shows a 26% drop in British applicants to EEE courses between 2002 and 2013. The not-for-profit organisation EngineeringUK called for more action to train and retain engineers, predicting a potential economic boost to the British economy of £27bn per year from 2022 – if demand for new engineering jobs was filled.

In a separate move – and out in Siberia, T&M giant Keysight Technologies has announced its cooperation with Tomsk State University of Control Systems and Radioelectronics (TUSUR), one of the leading technical universities in Russia, in setting up a Center of Competence to advance students' understanding of RF and microwave technologies.

Part of the programme involves a new RF and microwave teaching and research lab, equipped with Keysight hardware and software solutions. This will be the first centre in the Siberian region to provide students with the opportunity to develop and enhance the skills they need to design, analyze and debug complex systems.

"This cooperation with Keysight Technologies will allow our students to gain important hands-on test and design experience," said Alexander Shelupanov, Provost for Research of TUSUR University. "This will help prepare the students for critical positions in industry, and our researchers will have access to the most advanced test and measurement instruments."

DESIGNSPARK

Brought to you by RS

Put innovation back at the heart of your design process

Our unique suite of tools and resources are custom-built to help get your big ideas from concept to prototype faster than ever before.

Perfect for product developers and electronics engineers, our tools give you back the time to indulge your passion for world-changing design.

Download our free and unrestricted suite of rapid prototyping tools at designspark.com

#RapidPrototyping

THIS SERIES PRESENTS THE RASPBERRY PI SINGLE-BOARD COMPUTER, ITS FEATURES AND BENEFITS, AND HOW TO USE IT IN VARIOUS PROJECTS

Connecting To A Wireless Network Via Wpa_gui

BY **GARETH HALFACREE**

The simplest way to connect to a wireless network from the Raspberry Pi is to use the wpa_gui tool. This provides a graphical user interface for software that would otherwise require the use of the terminal; it is accessed from the desktop by double-clicking the icon labelled WiFi Config.

The main wpa_gui window (Figure 1) has two drop-down lists, labelled Adapter and Network. The first should already be filled with the wireless network dongle's identifier, wlan0. If more than one dongle is connected, the one to configure is easily selected. If nothing is listed, it's worth turning back a few pages to ensure the firmware for the dongle is correctly installed.

Finding a wireless network is a process known as scanning, which in wpa_gui is activated by clicking the Scan button at the bottom-right of the window. A second window pops up showing the results of the scan (see Figure 2). The name of your wireless network should show up; it should also be the strongest on the list. It will appear in the signal column, selected by a double-click.

The window that appears upon double-clicking the network asks for several different settings, depending on the type of network you are trying to connect to. For an unencrypted network – a bad thing to be running as it allows anybody within range to use your network – wpa_gui will require no additional settings; just click the Add button at the bottom.

Networks' Encryptions

If your network uses encryption, you need to choose the type of encryption, using the Authentication and Encryption

Figure 1: The wpa_gui application

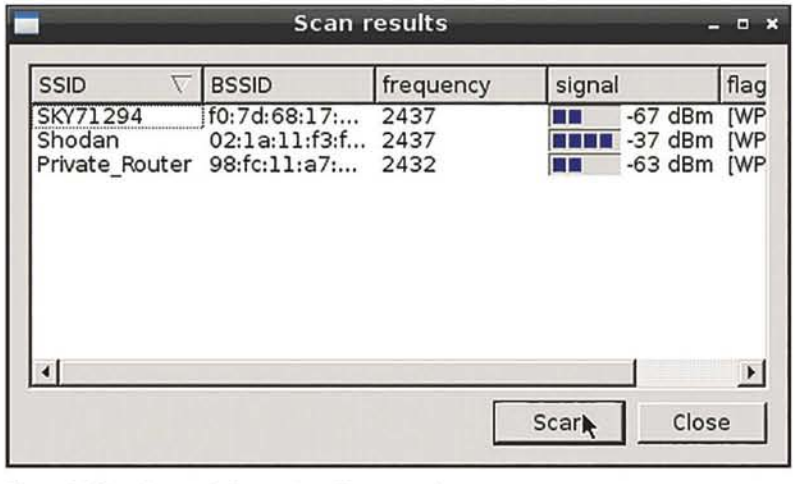

Figure 2: Choosing a wireless network in wpa_gui

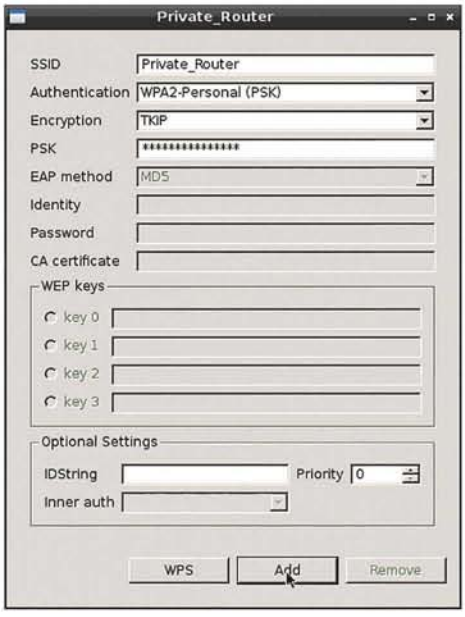

Figure 3: Adding a network to wpa_gui

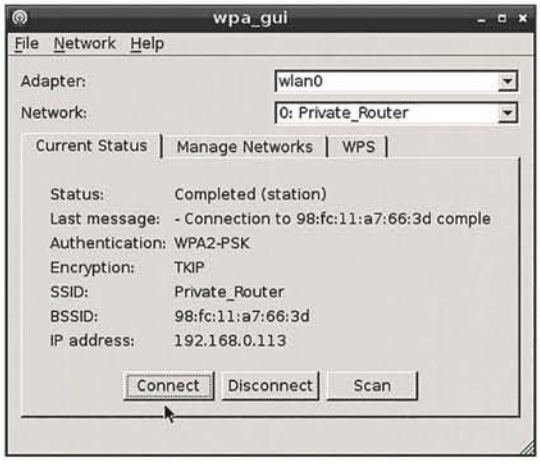

Figure 4: Connected to a wireless network via wpa_gui

drop-down lists (Figure 3). In most cases, wpa_gui will have selected these values automatically. If so, the password known as a pre-shared key should be typed in the box labelled PSK; then click the Add button.

If the network encryption is Wired Equivalent Privacy (WEP) rather than the more secure Wireless Protected Access (WPA) type, at least one key must be filled in the WEP keys section. If an authenticated enterprise network is used, details of your identity, password and encryption certificate can be added, but most home users will not need these fields.

If the network includes a Wi-Fi Protected Setup (WPS) option, the WPS button should be clicked for a simple setup. Simply press the WPS button on your router or access point and then click the WPS button in wpa_gui to connect automatically.

After the details of your network are filled in, click Add. This step closes the window and returns to the main wpa_gui window, but now the Network drop-down should have an entry, named after your wireless access point. At this point, wpa_gui automatically connects you to the wireless network and an IP address should appear at the bottom of the screen (see Figure 4).

If you need to connect to a different network in the future, simply start the process again from the beginning. Connecting to a new network won't cause wpa_gui to forget the old network; both will appear in the drop-down list, and you can connect to any network within range simply by choosing it from the list, once the network has been configured.

You can also use wpa_gui to disconnect from a wireless network without having to physically remove the wireless dongle. Simply click the Disconnect button at the bottom of the main window, and after a few seconds your Pi should be removed from the network. To reconnect, click the Connect button.

Connecting To A Wireless Network

If the Pi is running without a graphical user interface, you can also connect to wireless networks at the terminal or console. First, check that the USB wireless adapter is working as it should by using the iwlist command to scan for nearby wireless access points (see Figure 5). This list will probably be larger than a single screen, so pipe the command's output through to pause after each screen:

sudo iwlist scan | less

This command returns a list of all the wireless networks reachable from the Pi, together with their details. If at this point an error message appears, in particular one that claims the network or interface is down, check that the correct firmware is installed and that the USB wireless adapter is connected to a powered USB hub.

The current status of the network can be checked with the iwconfig command. Like ifconfig, the iwconfig command allows checking the status of a network interface and issuing configuration commands. Unlike ifconfig however, iwconfig is specifically designed for wireless networks and includes specific features for this. Type the command iwconfig at the terminal.

To connect the Pi to a wireless network, you need to add some lines to the /etc/network/interfaces file.

First, open the file in the nano text editor: sudo nano /etc/network/interfaces.

At the bottom of the file, create a new entry for the USB wireless adapter that reads:

auto wlano
iface wlano inet dhcp
wpa-conf /etc/wpa.conf

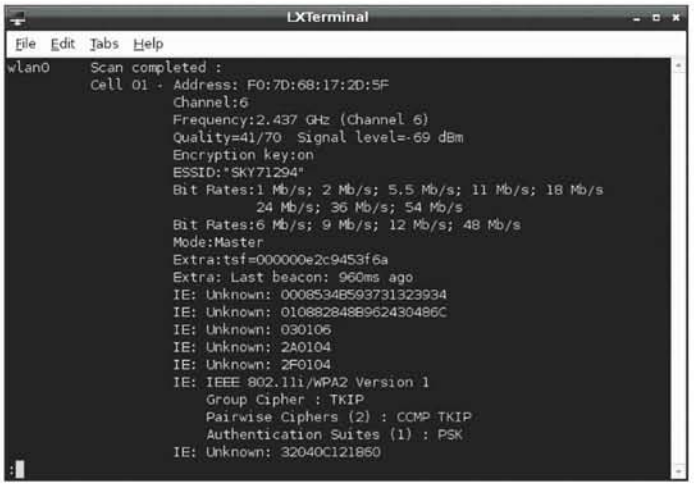

Figure 5: Scanning for wireless networks with iwlist

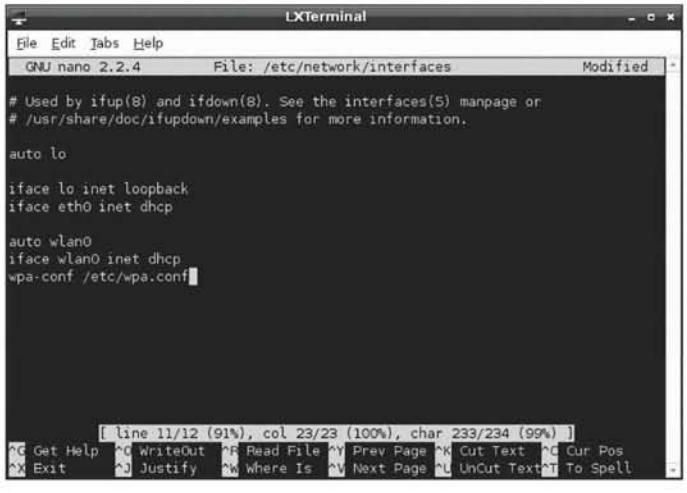

Figure 6: Editing the interfaces file for wireless network access

Once the entry is in place, save the file by pressing Ctrl+O and then quit nano with Ctrl+X. The last line of the interfaces file makes reference to a configuration file, wpa.conf, which does not yet exist (see Figure 6). This file is used by a tool known as wpasupplicant, designed to provide Linux with an easy way to connect to networks secured with the Wireless Protected Access (WPA) encryption.

Using wpasupplicant, you can connect the Pi to almost any wireless network, regardless of whether it's protected by WPA or its newer replacement, WPA2, in both Advanced Encryption Standard (AES) and Temporal Key Integrity Protocol (TKIP) modes.

Despite its name, wpasupplicant also permits connection to wireless networks using the older Wired Equivalent Privacy (WEP) encryption standard.

The wpasupplicant program stores its configuration in a file called wpa.conf, located in the /etc directory. To begin configuring the Pi for wireless access, first open a new blank file for editing by typing:

sudo nano /etc/wpa.conf

Enter the following two lines, which, again, are the same for any wireless network type; replace Your_SSID with the SSID for the wireless network to which you want to connect and then finish the file with the lines that match your network's encryption type:

network={
***Tab]* ssid=" *Your_SSID*"**

At this point in the configuration file, the details required differ depending on the type of wireless network you are configuring to join. ●

RASPBERRY PI USER GUIDE

Gareth Halfacree is co-author of the Raspberry Pi User Guide with project co-founder Eben Upton.

Halfacree often reviews, documents and contributes to projects such as GNU/Linux, LibreOffice, Fritzing and Arduino. He is also the creator of the Sleepduino and Burnduino open-hardware projects, which extend the capabilities of the Arduino electronics-prototyping system.

We have copies of the Raspberry Pi User Guide to give away at the end of the series. Register your interest by writing to the Editor at svetlanaj@sjpbusinessmedia.com, mentioning the title of the book in the heading.

RADIOMETRIX

www.radiometrix.com

Frequency Programmable Narrow Band Transmitter

New range of highly flexible, frequency programmable, RF power adjustable radios.

True Narrow Band FM performance, available on user/factory programmable custom frequencies between 425MHz & 470MHz. Matching receiver available.

VISIT http://radiometrix.com/content/ntx2b

CALL +44 (0)20 8909 9595 *REAL RADIOS FOR REAL APPLICATIONS*

The Thrill Of Touch

LUCIO DI JASIO, ELECTRONICS ENGINEER AND TECHNICAL AUTHOR, PRESENTS THIS SERIES ON EMBEDDED USER-INTERFACE DESIGN ON A BUDGET

One relatively recent innovation in user interfaces is the ubiquitous use of touchscreens. This has come to prominence with mobile phones and tablets and is now making its way to laptop and desktop computers, although not without some challenges. In fact, the main question to ask every time a new tool is made available is: "Does it really help solve a problem?"

In the case of mobile phones and tablets, where space is at a premium, replacing a fixed keyboard is a big help; in the case of laptops and desktops I am not so sure, and in the case of embedded applications the answer might be: "It depends!"

Resistance

Depending on the application and the specific touchscreen technology used, having to touch a screen in order to provide an input might actually cause problems. Think for example of a welding machine. What if the operator's hands are dirty? What if thick gloves are worn? Probably a fancy high-resolution multi-touch (projective capacitive) touchscreen is not the right answer. A few hard buttons and possibly a knob or two would serve better. But there are also simpler and more robust resistive touchscreen technologies that might help change opinions.

A resistive touchscreen is less sensitive to dirt and other surface contaminants; it can be used with gloves, and while it does not allow multi-touch detection, it does make up for it with very low cost and low complexity.

The best approach is not to fall for the hype (yet!), and select the right tool for the job on a case-by-case basis.

The Microchip Library for Applications (MLA), and in particular its graphics library, can handle any kind of touchscreen technology thrown at it, as long as touch inputs are enabled in the GraphicsConfig.h file by un-commenting the corresponding line:

```
...
#define USE_TOUCHSCREEN                 //
Enable touchscreen support.
//#define USE_KEYBOARD                  //
Enable key board support.
...
```

Support is provided 'out of the box' for traditional 4-wire resistive touchscreens (see Figure 1) connected directly to the microcontroller via a driver (TouchScreenResistive.c located in the MLA Board Support Package folder) that can simply be included in the project source files list. Once the physical connections to the

Figure 1: Typical touchscreen display

Figure 2: Simplified structure of a resistive touchscreen

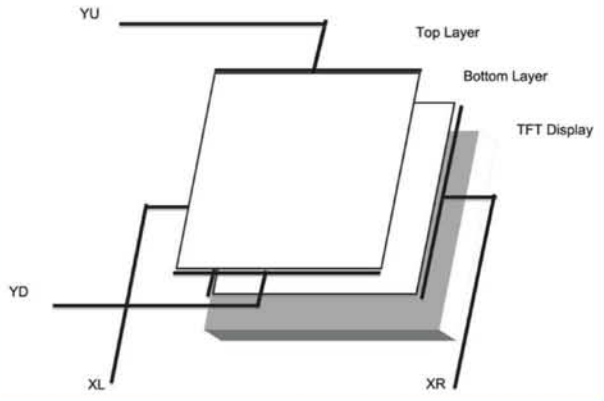

Figure 3: Mikromedia board, touchscreen interface detail

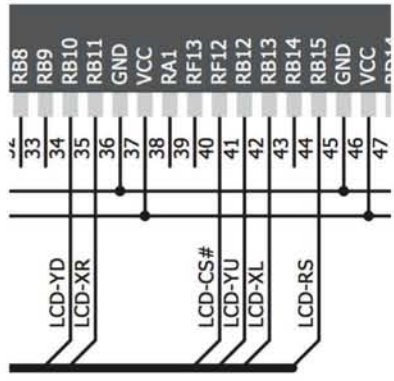

MCU are defined (see Figure 2), two ADC inputs and two digital outputs are needed, which can be added to the Hardware Profile:

```
...
// Analog inputs definitions
#define ADC_XPOS 13
#define ADC_YPOS 12
#define ADPCFG_XPOS AD1PCFGbits.PCFG13
#define ADPCFG_YPOS AD1PCFGbits.PCFG12
...
// X port definitions
#define ResistiveTouchScreen_XPlus_Drive_High()
LATBbits.LATB13 = 1
...
#define ResistiveTouchScreen_XMinus_Drive_High()
LATBbits.LATB11 = 1
...

// Y port definitions
#define ResistiveTouchScreen_YPlus_Drive_High()
LATBbits.LATB12 = 1
...
#define ResistiveTouchScreen_YMinus_Drive_High()
LATBbits.LATB10 = 1
...
```

And since this is exactly how Mikromedia (and most of Microchip's own) development boards touchscreens are configured, we are ready to go at the touch of a button.

If higher resolution touchscreen display controllers or (projective capacitive) touchscreen controllers are used to assist the MCU, all that's needed is to modify the hardware profile accordingly to define the specific interface (I2C, SPI, ...) and replace the Board Support Package driver with another one, or possibly write our own. This will need a suitable TouchDetectPosition()function for the graphics library to call upon.

Cold Fingers

Regardless of the technology used, there is often a need to adjust the touch sensor input to changing environmental conditions. Temperature variations affect resistive touchscreens, and moisture and various contaminants can affect capacitive sensors. The result is having to calibrate the display – adjustment of the mapping between the position of the touch point on the screen and the coordinates passed to the graphics library. Modern displays are quite well compensated and otherwise require rather small adjustments, unless a very high resolution is expected.

Specific Conditions?

This brings us to another important point: How small do you expect user hands to be? Or do you expect the user always to reach for a stylus?

Once again mobile phone and tablet designers have been ahead of the rest, figuring out that (similarly to a previous article's considerations about the choice of proper spacing and layout to help with focus) the best user interface is one with fewer and larger buttons.

Styluses are great for artwork, but do they really have a role in a welding machine user interface?

The MLA Touch Support

The MLA touch support example modules do suggest a simple 4-point calibration procedure that is enabled automatically during initialization of the graphics library: "tap here, here, here, confirm, done!"

This is handy, but I assure you it will get to your nerves really quickly during development. Every single time you reset the application or start a new debugging session, the graphics library will ask to repeat the calibration sequence, again and again.

Wouldn't it be nice to have the option of making the calibration less "volatile"?

This is also covered by the MLA examples, but it brings up the topic of interfacing to external non-volatile memories, which have their own complexities and will be explored in a future article.

GOL Or Grid

The universally-recognized, proper way to handle touch inputs in a Graphical User Interface (GUI) is by implementing a fully event-loop-driven application. This might include buttons, entry fields and any number of touch responsive widgets, as encountered with IOS, Android and similar user interfaces. If that is what your application needs, then you are in luck, since the MLA provides a small but effective library, the Graphics Object Layer (GOL), that relies on the underlying graphics library and provides a selection of approximately twenty basic widgets (objects) to use and build upon. Except that, for some applications this could be overkill or too disruptive.

When upgrading a legacy application that previously relied on physical buttons and possibly alphanumeric displays, adopting the pure event-driven application structure required by GOL could be too expensive. In my book "*Graphics, Touch, Sound and USB. User Interface Design for Embedded Applications*" I suggest a much simpler alternative for such cases: use a simple fixed grid.

In Closing

Touch can be a viable way to capture user inputs in embedded applications; just don't get carried away with it and make sure you choose the right technology for the application. Robustness can be just as important as resolution, or more so.

Resistive sensing technology, although basic and less flashy than modern alternatives, can be the right choice when we understand the environment and the uses. ●

USER INTERFACE DESIGN FOR EMBEDDED APPLICATIONS

Lucio Di Jasio is EMEA Business Development Manager at Microchip Technology. He has held various technical and marketing jobs within the company's 8, 16 and 32-bit divisions for the past 18 years. Lucio has published several books on programming for embedded control applications, and we have three copies of his book *'Graphics, Touch, Sound and USB, User Interface Design for Embedded Applications'* to give away at the end of the series. If you want to win, please send an email to svetlanaj@sjpbusinessmedia.com, mentioning the book in the heading.

Now, lower your operating costs without compromising availability.

With three modes of efficiency, the new Galaxy VM delivers the performance you need.

Balancing the trade-off between availability and efficiency has always been a challenge. The Galaxy™ VM three-phase UPS from Schneider Electric™ eliminates this issue, with three modes of efficiency to deliver the highest availability. The exclusive ECOnversion™ mode provides 99 percent efficiency, offering higher cost savings and reduced risk while retaining the power conditioning of double conversion. Innovative modular battery architecture lets you pay as you grow, increasing capacity and runtime with flexible energy storage.

Trusted partner for your business continuity

Seamlessly integrating with the electrical networks, physical infrastructure, and monitoring systems in any data center, and boasting one of the industry's most compact footprints, the unit fits almost anywhere with minimal space requirements. Also featuring isolated connections and bypass cabinet completely separated from power for safe service and easy maintenance, top and bottom cable entry, and included start-up service, the Galaxy VM is one of the easiest UPS units in its class to deploy, install, and maintain.

Business-wise, Future-driven.™

Easily serviceable, cost-saving design

Three modes of efficiency:
The only UPS on the market with three modes of efficient operation to deliver the availability and performance your business needs.

Modular battery architecture:
Pay-as-you-grow modular energy storage offers increased availability and scalability.

Front-access servicing:
Quick and easy installation and maintenance, reduced mean time to repair, and valuable floor space savings.

Equipment life cycle services:
Schneider Electric Critical Power & Cooling Services offers monitoring and maintenance services to protect the health of your Galaxy VM.

Download our white paper
"Calculating Total Power Requirements for Data Centers"

Visit: www.SEreply.com Key Code: · · · · · · Call 0845 0805034 · Fax 0118 903 7840

Schneider Electric™

Test Your Modem

BY **MYK DORMER**

Low-power radio links can be tricky to use. The interfaces can be awkward, the data path – or sometimes it's the raw baseband path – can be noisy and intolerant of data waveform asymmetry, and the timing characteristics of the radio hardware can be inconvenient and exacting. To many users the ideal would be a device that replicates a simple serial cable, and that is precisely the functionality that a radio modem provides – or tries to.

Until it doesn't work.

Behind their easy-to-use interfaces, radio modems are actually conducting some fairly sophisticated data processing. To connect a user's generic datastream to the radio, the modem buffers the incoming data, formats it into carefully formatted packets, adds framing/sync information, error handing (checksums or CRCs) and often addressing and routing data. This air-interface-compatible data is then presented to the transmitter in accordance with its timing and bandwidth requirements, and at the receive end the entire process is reversed to regenerate a plausible copy of the input datastream, albeit after an unavoidable processing and transmitting delay, or "latency" time.

> Behind their easy-to-use interfaces, radio modems are actually conducting some fairly sophisticated data processing

It's no surprise that this process sometimes goes amiss.

There are a fair number of ways that a radio modem can fail: there can be a total loss of communication (in one or both directions); data communication can become intermittent or parts of a message lost; timing can become compromised or data latency becomes unexpectedly long; or, in certain extreme instances, the data passes successfully but the modem activity – in terms of transmit burst length or the behaviour of the unit's data-flow indicators – looks aberrant.

Diagnosing such problems has to be a process of elimination, and will require some bench effort and test equipment. Just what hardware is available to the user (and what indicators and readouts are present on the modem) will predicate which tests can be conducted, bearing in mind that some investment in basic diagnostic equipment is necessary: there is no "magic wand", and nothing can be fixed by just looking hopefully at the blinking lights.

Substitution testing should be the first step. Unless something very complex is being done (dynamic address point-to-multipoint for example, or different user interface data rates at different ends of the link), it ought to be possible to replace the misbehaving modems with a simple serial cable. If the user's system misbehaves over a cable, then the radio modems are not the problem. If an RS232 analyzer or breakout box is available at this stage, it will pay dividends, as it gives a clear indication of the overall patterns of serial bus activity.

Replacing the user hardware at one end of the link with a PC running a simple terminal program (or, if available, a serial communications analysis program) will allow the data baud rate and format to be checked (and matched against those required by the modem) and the expected data output of the user system to be monitored.

Putting a substitute PC at both ends of the modem link (running terminal emulators, or simple communication test programs) will allow the radio modem link to be exercised and aberrant behaviour examined completely separate from the user system. Again, if the modems function correctly with simulated datastreams, but fail in the end user system, then the fault may not be in the modem.

Examination of the modem setup should come next. If the cable substitution test finds no issues with the overall data structures, then it is possible that the modem is set up incorrectly. Complex units, with many different modes and options, are actually more prone to this issue than simple, "fixed data rate, fixed-timing, point-to-point" devices.

With the exception of a few older devices (set up using hardware jumpers or DIP switches), most radio modems have some form of "configuration" screen or defined setup protocol to allow the user to set up many of the modem's parameters. It is absolutely vital that these values match both the modem's radio hardware performance and the user's interface parameters.

The simplest defect here is a mismatch in serial baud rate or handshaking. Following this, the modem's radio channel frequency must be correct, and (if provided) so must its unit address. Many modems also allow the basic timing parameters to be edited by the user. If the preamble (TX setup time) is set too short, then bursts will be lost as the vital framing sequences at the start of the transmissions will be corrupted.

Incorrect values in other timing parameters, such as the delay between "first byte received" and transmission burst start, can also cause trouble, through unexpectedly long latency times or buffer overflows. Returning to the manufacturer's recommended defaults can often be useful.

Some modems also have advanced modes (network operation, acknowledge/resend modes, repeater functions), which, while valuable in their place, may cause some very odd behaviour if inadvertently selected.

Finally, if all the simpler tests have yielded null results, proper bench hardware tests need to be conducted. This is necessary when the modem hardware, or the user hardware, is suffering from some form of defect outside its usual operating mode. These effects can be quite subtle. Examples include:

- RF energy from the modem's aerial (or even radiating from a badly terminated feed-line) getting into the user hardware, resetting or triggering circuitry.
- Power supplies can fail under (usually transmitter current) load, causing brownouts, resets, glitches or software crashes.
- Logic voltages at the modem's user interface may be out of specification, or may have the wrong sense or function.

Hardware tests require at the least a good oscilloscope to monitor voltage levels and to observe datastreams. A logic analyser or combination scope/analyzer can be even more useful, to simultaneously monitor and log multiple data signals. A simple multimeter or logic probe will probably not be sufficient for anything but steady state power supply tests.

If RF test equipment is also to hand, a modulation analyzer (and/or spectrum analyzer on zero span) will permit monitoring the envelope, content and timing of the modem's RF transmit burst.

If all possible tests have been exhausted without finding a solution, then the modem manufacturer's support engineers may be able to help further, but please remember that we are not magicians, and the more detailed the fault descriptions and test results you give us, the faster and more efficient our responses – and hopefully solutions – will be. ●

Myk Dormer is a Senior RF Design Engineer at Radiometrix Ltd
www.radiometrix.com

HIGH DEFINITION CAMERA DEPLOYMENT USING SUPERSPEED USB INTERCONNECT TECHNOLOGY

By Fred Dart, FTDI Chip

High definition (HD) video offers improved picture quality, greater colour depth, increased frame rates and superior contrast over traditional video technology. It has, as a result already seen widespread adoption in home entertainment applications - effectively becoming almost ubiquitous here. There are however a vast array of other places where its employment could prove to be advantageous in the future. The following article will look at how the advent of the USB 3.0 interface could open up new opportunities for HD video implementation.

Some of the sectors that could majorly benefit from HD video implementation include factory automation, surveillance and healthcare. All of these are likely to require the rapid identification of objects, and are therefore in need of a combination of high frames rates and strong image clarity. The envisaged video imaging systems serving these sectors must however still maintain a high degree of cost effectiveness too. USB 3.0 (SuperSpeed) has characteristics that make it very attractive for such implementations. In addition to supporting ultra-fast data transfer, it is also capable of doing so over distances of 10 metres (while other interface technologies are often limited just a few metres). Implementation of video imaging hardware via this method also makes use of the power delivery element that USB technology bestows. This eliminates the need for separate cable feeds for power and data - thereby lowering the overall deployment cost, as well as saving space.

USB ports first became popular during the mid-1990s. At that stage these were merely a means by which low data rate connectivity could be delivered to peripherals (such as mice, keyboards, printers, etc.). Since then USB has continued to progress, and today there are estimated to be in the region of 7 billion ports in operation globally.

The USB 3.0, though originally ratified back in late 2008, is now starting to feature in electronic system designs. Global Industry Analysts has predicted that worldwide annual sales of USB 3.0 enabled devices will ramp up quickly reaching the 3 billion units mark by 2018. The impetus behind this will of course be to meet demands for higher speed data transmission between electronics hardware - in particular transmission of video material. USB 3.0 pushes the performance envelope significantly - boosting the data speeds that can supported by an order of magnitude compared with the previous USB incarnation (USB 2.0), as well as bringing other functional benefits. Nevertheless it offers the same plug-and-play functionality that engineers have come to expect. Figure 1 compares USB 3.0 with USB 2.0 and Camera Link interfaces. It details how this latest interface technology allows the bottlenecks that have previously been experienced when transferring video content to be removed completely.

Proliferation of HD video technology will call for a new generation of interface ICs. Figure 2 describes an imaging system utilising USB 3.0. Running on the Windows 8 operating system, it incorporates a high resolution microscope camera (2560 x 1440 pixels) from which imaging data is streamed to a QHD monitor via a USB 3.0 interface. The data transfer speed of 2.08Gbit/s means that a full resolution frame rate of 38fps can be sustained without any lag or image distortion occurring. As well as enabling consistently higher data rates than a USB 2.0 solution could deliver, this system can also benefit from the elevated power levels supported by the USB 3.0 specification - 900mA while still transferring data at top speed (compared with 480mA for USB 2.0).

The high data transfer capacity of the system described here stems from FTDI Chip's new FT601Q SuperSpeed USB-to-FIFO bridge interface IC. The camera control and data capture

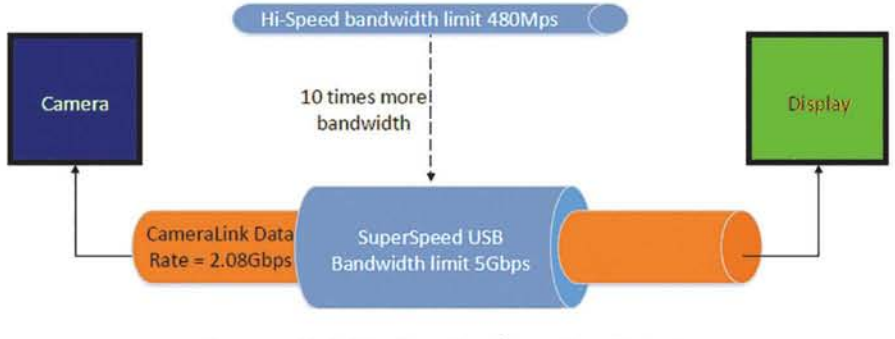

Camera Link Medium Configuration Data Rate

2560 x 1440 pixels x 16 bits/pixel x 38 FPS = 2.08Gbps

Figure 1: USB 3.0, USB 2.0 & Camera Link interfaces technologies are compared

Figure 2: Schematic of a video imaging system employing USB 3.0 technology

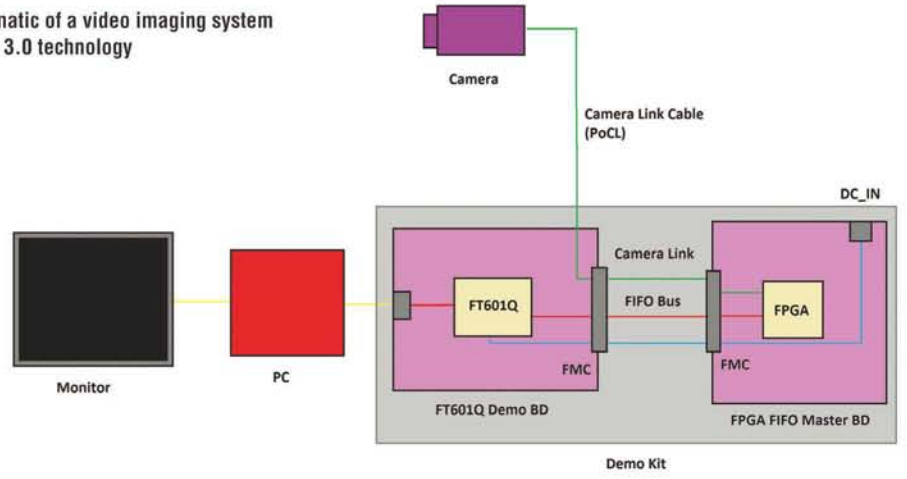

functions of the system are both handled by the accompanying FPGA device (a Xilinx Spartan 6 is used in this example). The FPGA takes care of the imaging system's timing functions (such as setting the frame rate, etc.). From there the acquired data is passed to the 32-bit parallel data bus incorporated into the FT601Q and subsequently transferred to the PC over the USB 3.0 interface before being displayed on the monitor.

Summary of items making up video imaging design example:

- Toshiba 2560 x 1440 pixel resolution microscope camera
- FTDI Chip FT601Q SuperSpeed USB-to-FIFO bridging IC
- Spartan 6 FPGA from Xilinx
- PC (incorporating a USB 3.0 port)
- QHD Monitor

Summary of FT601Q from FTDI Chip:

- 3.0 SuperSpeed USB-to-FIFO bridge
- Integrated 32-bit FIFO bus
- Hardwired microprocessor with proprietary 32-bit core running at 100MHz
- Supports USB bulk transfers
- 1 physical channel & 4 multiplexed logical channels
- 16kByte Tx & 16kByte Rx endpoint buffers
- Configurable 16kBytes FIFO buffer
- Can configure up to 10 separate USB endpoints
- Offered in QFN-56 and QFN-76 packages
- D2XX drivers for Windows, Linux & Mac platforms (with optimised data structures for performance/efficiency)
- Supports power management, suspend & remote wakeup

A single physical channel plus 4 multiplexed logical channels have been integrated into the FT601Q. Two modes of operation are provided. The first is a 245 synchronous FIFO legacy mode similar to that seen in earlier FT232H devices but with a 32-bit interface. The second is an enhanced FT600 FIFO mode catering for 4 discrete channels. The separate logic channels have 8-bits lengths, with each allowing for a full-32 bit interface to be created, but supporting asymmetric transfers. So that simplified implementation is assured, the various internal sub-units of the interface IC are controlled by its hardwired processor. This is based on the proprietary FTDI Chip 32-bit core, which runs at 100MHz. The multifaceted memory resource available to this core includes a 64kByte on-chip shadow program memory as well as 8kBytes of on-chip data RAM.

Through the embedded microprocessor resource of the FT601Q, engineers are presented with the design flexibility they need for configuring this USB 3.0 solution so that it matches their particular application requirements. Up to 10 separate USB endpoints can be configured, so that more than sufficient headroom is made available to engineers to create composite devices if needed. A completely new driver architecture has been developed to support designs where there are 8 or more data endpoints involved. It is optimised to extract full performance from the system whilst maintaining FTDI Chip's standard D2xx API. This driver support permits the device to be used with Windows, Linux and Mac operating systems.

USB 3.0 could prove to be the catalyst that leads to large scale uptake of HD video in non-consumer applications. It enables a dramatic reduction in implementation costs when compared to other data interface solutions, as well as avoiding heavy investment of engineering resources. Furthermore it means system designs are not dependent on niche technologies that are less commonly understood by engineers. Through utilisation of USB 3.0 the higher frame rates and crisper images desired for modern system implementations can be achieved without major financial outlay in the associated electronics hardware or allocation of large amounts of time and effort.

Figure 3: FTDI Chip FT601Q SuperSpeed USB bridging IC

ULTRA LOW VOLTAGE AND POWER DESIGN OF A 0.18um CMOS LNA FOR 4-5GHz APPLICATIONS

WEN WANG, CHUNHUA WANG AND **JIANQUN DING** FROM HUNAN UNIVERSITY IN CHINA

PRESENT A LOW NOISE AMPLIFIER SUITABLE FOR ULTRA-LOW-POWER AND ULTRA-LOW-VOLTAGE ULTRAWIDE BAND APPLICATIONS

Since 2002, when the US Federal Communications Commission (FCC) allocated the 3.1-10.6GHz frequency band for ultra-wideband (UWB) radios and authorized the technology for commercial use, there's been growing interest and research in UWB systems. Six years later, in December 2008, in China, the Ministry of Industry and Information Technology (MIIT) allocated the 4.2-4.8GHz frequency band for UWB applications too. The high data rate, low power and reduced interference makes UWB technology very attractive for commercial use.

LNAs

Part of the wireless receiver is the low noise amplifier (LNA) – a crucial element of the whole system. As the first section after the antenna, it has to meet several stringent requirements. For a UWB LNA these are: full bandwidth matching, low noise figure (NF), sufficient power gain and acceptable gain flatness. In addition, due to the large variety of wireless applications, low voltage and low-power requirements are becoming crucial considerations in LNA design, because of the limitations of battery capacity.

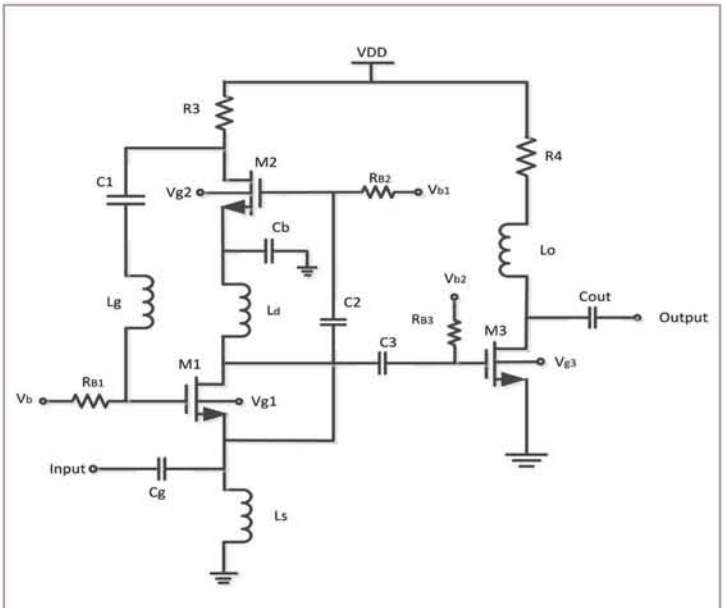

Figure 2: Schematic of the proposed UWB CG-LNA

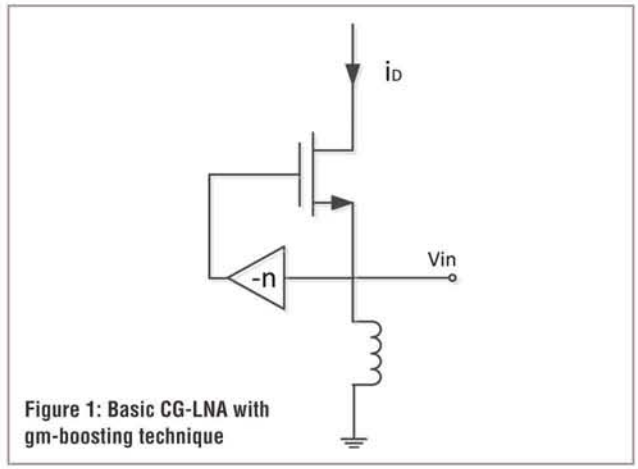

Figure 1: Basic CG-LNA with gm-boosting technique

There are several low-power CMOS LNA designs for UWB receiver systems that already exist. The conventional distribution amplifier (DA) absorbs the parasitic capacitance of the input transistor as part of the transmission line, which provides good operating performance over a wide range of frequencies. However, their large size makes them less attractive for low-cost applications and their relatively high power consumption is still a limitation for ultra-low-power designs.

Resistive feedback topology is a well-known technique used in wideband amplifiers. It provides broadband matching and flat gain over the entire bandwidth; nevertheless, it does not satisfy gain and noise requirements simultaneously.

Devices	Design Values	Devices	Design Values
M1(w/l)	45μm/0.18μm	RB2	4KΩ
M2(w/l)	35μm/0.18μm	RB3	7KΩ
M3(w/l)	42μm/0.18μm	C2	2pF
Cg	0.8pF	R4	40Ω
Ls	3nH	Lo	1.2nH
Lg	2nH	COUT	1pF
Ld	10nH	Vb	0.6V
RB1	1kΩ	Vg1	0.1V
Cb	3pF	Vg2	0.1V

Table 1: Summary of instance parameters

Passive filtering has been widely used to extend amplifier bandwidth. By adding a passive LC network in the conventional cascode structure, the narrow-band LNA can become a UWB LNA with good performance in power gain, input matching and noise figure. But the stacking of MOS transistors requires high voltage, so this is not suitable for ultra-low voltage designs. Meanwhile, more inductors in the LC filter add to the total area, which leads to higher costs.

Another popular wideband topology of interest due to its simplicity is the common-gate amplifier. Through proper setting of the transconductance of the input transistor, wideband matching and gain can be achieved, but due to parasitic capacitance the noise figure and gain deteriorate significantly. Gm-boosting is a good way to solve this problem. However, the additional gm-boosted stage adds to the power dissipation.

Here, we propose a novel current reuse gm-boosted structure, where the UWB LNA uses a common source (CS) amplifier as the gm-boosting stage which shares the bias current with the CG amplify stage. Besides employing a forward body bias technique, the operation voltage is effectively reduced.

It is shown that the UWB LNA exhibits enhanced RF performance at reduced voltage and lower power dissipation, which makes it very suitable for ultra-low-power and ultra-low-voltage applications.

Circuit Implementation

Based on current-reused CG configuration, we designed an ultra-low-power gm-boosted UWB LNA. Due to the relatively high quality factor Q, the CS-LNA cannot meet the UWB matching requirements without the help of other techniques. The CG-LNA, however, can easily achieve broadband impedance matching without many additional components, saving on chip area. Besides, the CG-LNA has better performance in linearity and lower power consumption. However, since the voltage gain of the CG-LNA is generally inferior to that of the CS-LNA, gm-boosting is utilized in this design.

The main disadvantages of a CG-LNA are the relatively high noise figure and weak amplifying ability. Neglecting the induced gate noise, the noise factor (NF) of the basic CG-LNA has a minimum NF:

$$F = 1 + \frac{\gamma}{\alpha} \quad (1)$$

where α and γ are bias-dependent parameters.

It is difficult for common-gate LNAs to provide a NF much below 3dB. Even worse, noise performance deteriorates significantly at high frequencies. The CG-LNA is incomparably superior in the input-impedance matching; however for an input of 50Ω, the required input transconductance has to be 20mS, which translates into high power consumption.

Gm-boosting is a good way to improve these issues. A conceptual illustration of the gm-boosting technique is shown in Figure 1, where an inverting replica signal with an amplitude n is provided from the source to the gate terminal. Consequently, the effective transconductance is boosted to:

$$g_{m,eff} = (1+n)g_m \quad (2)$$

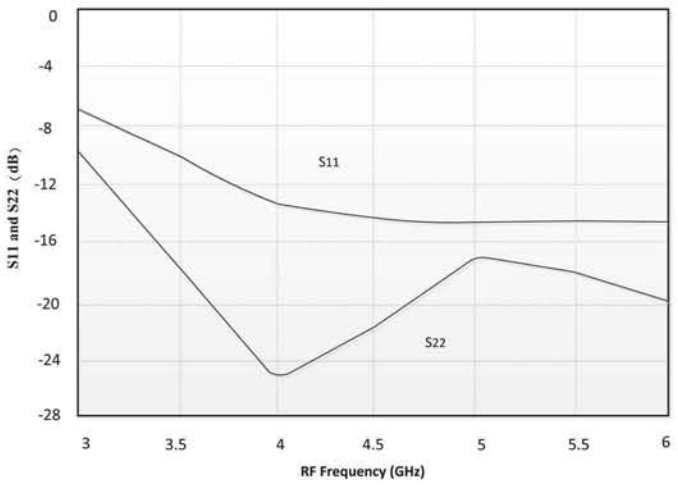

Figure 3: S11 and S22 of the proposed LNA

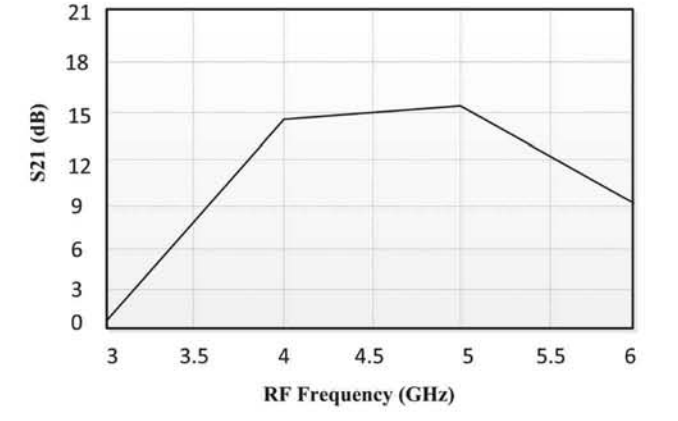

Figure 4: Simulated S21 of the proposed LNA

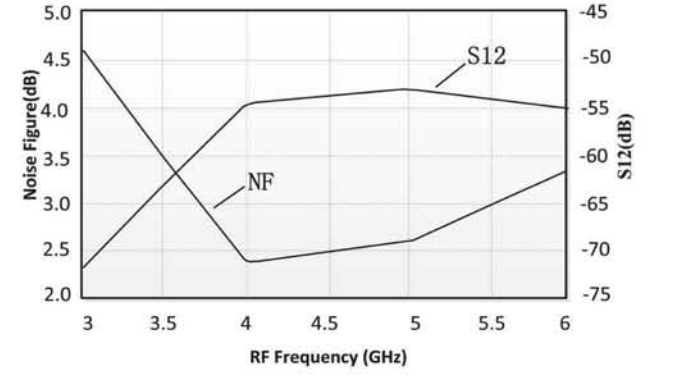

Figure 5: Noise figure (NF) and S12 of the UWB LNA

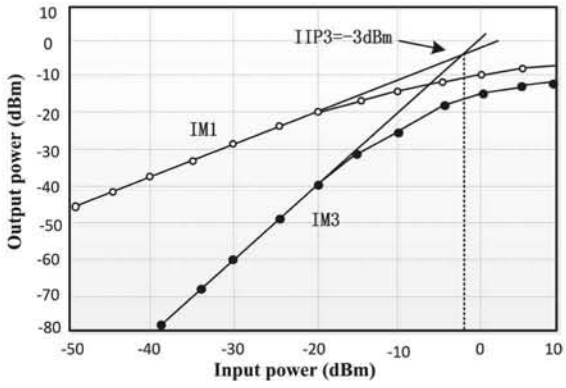

Figure 6: Input third order intercept point (IIP3) of the proposed LNA at 4.5GHz

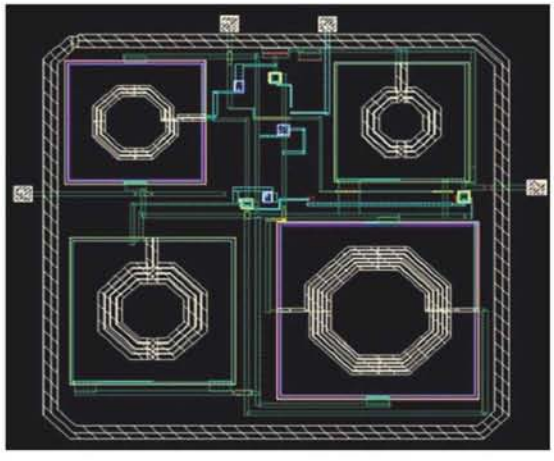

Figure 7: The layout diagram of the UWB LNA (0.8mm×0.8mm)

Correspondingly, the NF becomes:

$$F = 1 + \frac{\gamma}{\alpha}\frac{1}{1+n}\Big|_{(1+n)g_m R_s = 1} \quad (3)$$

In the literature, there are several methods for gm-boosting, achieved either with passive transformers or active circuits. Capacitive cross-coupling boosts transconductance by 2, nevertheless the differential architecture makes this configuration complex and, hence, doubles the power consumption.

The transformer structure is easy to implement, but it is not suitable for adoption in UWB applications due to process nonlinearities, and the NF may be deteriorate due to the parasitic resistance of the inductors.

There is a gm-boosted CG UWB LNA method that uses an active CS stage to provide the inverting gm-boosting gain. Compared with other topologies, the inverting amplitude provided by an active amplifier circuit is much larger, but the CG stage and gm-boosting circuit are separately biased at different DC paths, increasing total power dissipation.

In this design, a current-reuse architecture with stacked CG stage and gm-boosting is used. To save on DC dissipation current, the bias current is shared between the gm-boosting (CS) stage and the amplifier (CG) stage. In addition, to relieve the high-voltage supply needed by the stacked structure, a forward body bias technique is adopted.

Forward Body Bias Technique

The most efficient method to reduce power consumption is through supply voltage scaling. However, performance of the cascade degrades significantly as the supply voltage decreases.

For this design, with two MOSFETs stacked in stage one, low supply voltage is not practical. If the supply voltage is only 1V, the NMOS transistors are still in their weak inversion region, which leads to increased noise. To solve this problem, a forward body bias technique is applied to reduce the threshold voltage (V_{th}). For a standard CMOS process, the threshold voltage can be manipulated by the DC bias at the body terminal, adding one more degree of freedom in circuit designs. Typically, the threshold voltage of an n-channel MOSFET is given as:

$$V_{th} = V_{th0} + \gamma(\sqrt{2\varphi_f - V_{bs}} - \sqrt{2\varphi_f}) \quad (4)$$

Thus, threshold voltage can be manipulated by V_{bs}, where V_{bs} is the source-to-body voltage, V_{th0} is the threshold voltage when $V_{bs} = 0$, γ is the bulk threshold parameter, and φ_f is a semiconductor parameter with a typical value in the range of 0.3-0.4V.

With the forward body bias technique, the MOSFETs can operate at a reduced bias voltage, while device characteristics such as gain, linearity and noise figure are maintained equivalent.

REFERENCE	THIS WORK	[1]	[5]	[6]	[11]	[13]
Tech (μm)	0.18	0.13	0.18	0.18	0.18	0.18
BW (GHz)	4-5	4.2-4.8	3-5	3.1-4.9	6-8.5	3.1-10.6
Vdd (V)	0.6	1.2	1.8	1.0	1.8	1.8
NF (dB)	2.3-2.6	2.3-3.7	3.8-3.9	4.5-5.0	3.95-6.81	3.1-6
IIP3 (dBm)	-3	-2	-10	-5	----	-7
S11 (dB)	<-12	<-9	<-10	<-5.6	<-10	<-9
S21 (dB)	14.5-15.3	28#	11	10.3*	14.3*	13.5-16
S22 (dB)	<-16	<-10	<-15	<-8.6	<-14.9	----
Power (mW)	0.9	21.6	5.6	2.39	5.26	11.9

Table 2: Table 2: Performance summary and comparison with other UWB CMOS LNAs
*** maximum power gain; # tunable maximum gain**

Circuit Design

A two-stage architecture is adopted in this design. The schematic of the proposed UWB LNA is shown in Figure 2. As the first stage, the CG with low input impedance characteristic and broadband behaviour provides a NF almost independent of the frequency of operation. Meanwhile, the CG stage also eliminates the Miller effect and, hence, provides better isolation from the output return signal.

In the gm-boosting inverting stage, the NMOS CS amplifier M2 is used to overcome the inherent low transconductance of the CG-LNA, which not only enhances amplification gain but also improves noise performance. To save on current dissipation, the CG-LNA and gm-boosting stage are biased at the same DC voltage. As a result, better UWB noise performance and input matching are accomplished without increasing power dissipation or device size.

A common-source amplifier, M3, is designed as the second stage, providing another stage of gain.

At the input stage, capacitor Cg and inductor Ls are part of the 50Ω input matching network, whilst the series resonant LC tank with Lg and C1 provide low impedance AC coupling paths for signals between M2's M2 and M1's gate. Capacitor C_b is a bypass capacitor so the high frequency AC current flows to ground, which avoids signal interference coupled back to M1. In addition, an inductor, L_d, is provided as an RF choke to isolate M1 and M2. The input RF signal is simultaneously fed to the M1 source and NMOS M2 gate to be amplified, then with a path through M2, an inverting signal is applied back to the gate of M1. Therefore, the equivalent transconductance ($g_{m,eff}$) of M1 is increased, which leads to the high NF character of the conventional CG-LNAs being reduced.

To ensure sufficient gain over the whole frequency range, a common-source amplifier is used in the second stage. The shunt peaking inductor (Lo) and resistor (R4) are used to achieve bandwidth extension. The design parameters for most instances in Figure 2 are summarized in Table 1.

Simulation Results

The proposed UWB LNA is simulated with Agilent ADS using the TSMC 0.18μm CMOS technology. Figure 3 shows the simulated input/output reflection coefficients, which are below -12dB and -16dB respectively. Figure 4 shows the S21 of the LNA, which ranges from 14.5dB-15.3dB with gain variation as small as 0.8dB.

Due to the superior reverse isolation performance of the CG-LNA, S12 is below -50dB, as seen in Figure 5, which also shows the NF of the LNA, 2.3dB-2.6dB over the desired frequency band. Figure 6 shows the linearity check; the IIP3 is -3dBm at 4.5GHz. Total power dissipation of the proposed UWB LNA is only 0.9mW at 0.6V.

The layout of the circuit is shown in Figure 7, which occupies a compact chip area of 0.8mm×0.8mm.

The performance of this proposed UWB LNA is summarized in Table 2, where comparisons with other, previously published CMOS UWB LNAs are also provided. From the table it can be seen that the proposed LNA achieves good matching, low NF and high voltage-gain, while at the same time operating at ultra-low voltage and power.

SIMULATION AND EXPERIMENTAL STUDY ON CANTILEVER PIEZOELECTRIC VIBRATION GENERATOR

TO IMPROVE THE OUTPUT OF A CANTILEVER PIEZOELECTRIC VIBRATION GENERATOR, **YAN ZHEN** FROM THE AGRICULTURAL UNIVERSITY OF HEBEI IN CHINA ANALYZES THE EFFECTS OF ADDING A MASS TO IMPROVE FREQUENCY AND OUTPUT VOLTAGE, VERY IMPORTANT FOR LOW-POWER ELECTRONIC DEVICES

MEMS (micro electro mechanical system) based cantilever piezoelectric vibration generators (CPVG) can be used to provide energy for electronic devices with low power consumption – particularly important in wireless sensor networks. But, CPVGs need specific working conditions, which has limited their widespread use. Studies have shown that power generated by a CPVGs is only half of its potential maximum, if its inherent frequency deviates from the environment frequency by as little as 2%. In addition, no energy can be derived from the CPVG if the inherent frequency deviates from the environment frequency by more than 5%.

To improve their capacity and make CPVGs more attuned to the environment, a tip-proof mass is attached at the free end of the CPVG to tune its natural frequency to the desired value.

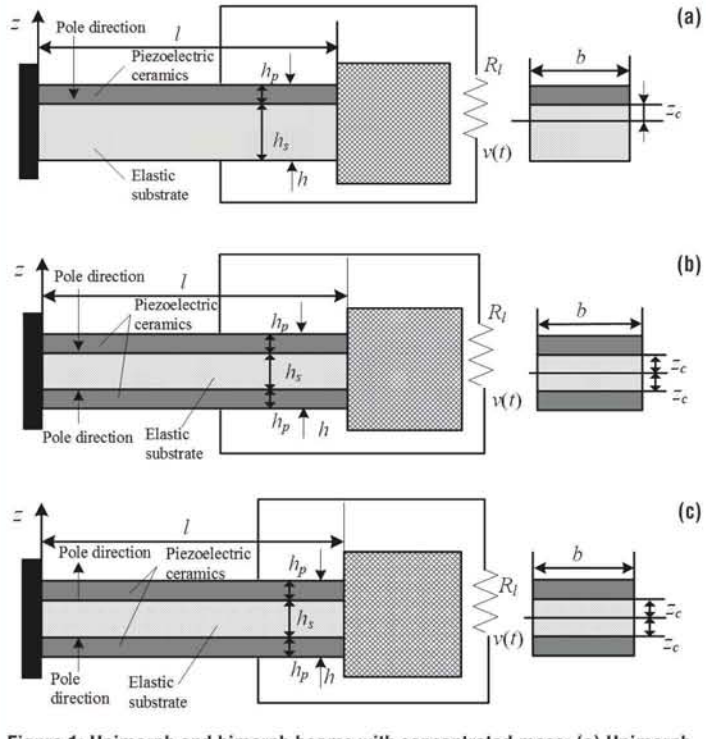

Figure 1: Unimorph and bimorph beams with concentrated mass: (a) Unimorph beam; (b) Bimorph-in-series type beam; (c) Bimorph-in-parallel type beam

CPVG Structure

CPVGs are formed of piezoelectric ceramic, electrode, elastic substrate and fixed support. The piezoelectric ceramics is tightly integrated into the substrate, with the electrode attached to it. One end of the generator is fastened to the support, and the other vibrates freely with the source. Because the generator's length and width are greater than its thickness (which is a thin-walled beam structure, meeting the theoretical requirements of a composite Euler-Bernoulli beam), the influence of the shear deformation and rotational inertia can be neglected; the transformation is regarded as linear under low amplitude conditions.

With continuous excitation, the piezoelectric ceramic moves and deforms in tune with the vibration source to generate charge, creating continuous current output at load resistance; thus mechanical vibration energy translates into electric energy.

Structures of the three main cantilever piezoelectric generators are shown in Figure 1. Figure 1a shows a unimorph beam structure; Figure 1b shows a bimorph-in-series type structure; and Figure 1c shows a bimorph-in-parallel type. The piezoelectric beam length is indicated by l, width by b, and thickness by h, with the superscripts s and p representing the substrate and piezoelectric layers respectively. Superscripts u, bs and bp represent unimorph, bimorph-in-series and bimorph-in-parallel beams respectively.

The added mass results in amplitude increase and CPVG vibration performance variation, so the influence of the mass on the normalization function and electromechanical coupling should be analyzed, and a mechanical model of the CPVG with mass established.

According to piezoelectric theory, when the free end of the CPVG is subjected to continuous bending and displacement by external forces, the surface of the piezoelectric beam generates free charge, with stress and electric field per the equations below:

$$\begin{cases} \{D\} = [d]\{T\} + [\varepsilon^T]\{E\} \\ \{S\} = [s^E]\{T\} + [d]^t\{E\} \end{cases} \quad (1)$$

where {D} is electric displacement, {E} is electric field

intensity, [d] is the piezoelectric constant matrix, {S} and {T} are the strain and stress, [ε^T] is the free dielectric constant matrix at constant stress, and [s^E] is the short-circuit elastic compliance coefficient matrix at constant electric field.

When the piezoelectric beam undergoes harmonic excitation – i.e. when the excitation frequency is close to the first-order inherent frequency – the steady-state voltage response and lateral displacement relative to the hold-down support of all three types are as follows:

$$\hat{v}_u(t) = \frac{j\omega R k_1^u F_1 e^{j\omega t}}{\left(1+j\omega RC_p\right)\left(\omega_1^2-\omega^2+j2\zeta_1\omega_1\omega\right)+j\omega R k_1^u \chi_1^u} \quad (2)$$

$$\hat{w}_{rel}^u(x,t) = \frac{\left(1+j\omega RC_p\right)F_1\phi_1(x)e^{j\omega t}}{\left(1+j\omega RC_p\right)\left(\omega_1^2-\omega^2+j2\zeta_1\omega_1\omega\right)+j\omega R k_1^u \chi_1^u} \quad (3)$$

$$\hat{v}_{bs}(t) = \frac{j2\omega R k_1^{bs} F_1 e^{j\omega t}}{\left(2+j\omega RC_p\right)\left(\omega_1^2-\omega^2+j2\zeta_1\omega_1\omega\right)+j2\omega R k_1^{bs} \chi_1^{bs}} \quad (4)$$

$$\hat{w}_{rel}^{bs}(x,t) = \frac{\left(2+j\omega RC_p\right)F_1\phi_1(x)e^{j\omega t}}{\left(2+j\omega RC_p\right)\left(\omega_1^2-\omega^2+j2\zeta_1\omega_1\omega\right)+j2\omega R k_1^{bs} \chi_1^{bs}} \quad (5)$$

$$\hat{v}_{bp}(t) = \frac{j2\omega R k_1^{bp} F_1 e^{j\omega t}}{\left(1+j2\omega RC_p\right)\left(\omega_1^2-\omega^2+j2\zeta_1\omega_1\omega\right)+j2\omega R k_1^{bp} \chi_1^{bp}} \quad (6)$$

$$\hat{w}_{rel}^{bp}(x,t) = \frac{\left(1+j2\omega RC_p\right)F_1\phi_1(x)e^{j\omega t}}{\left(1+j2\omega RC_p\right)\left(\omega_1^2-\omega^2+j2\zeta_1\omega_1\omega\right)+j2\omega R k_1^{bp} \chi_1^{bp}} \quad (7)$$

In these equations, R indicates load resistance, k_t is the modal coupling term, F1 is the excitation function amplitude, C_p is the piezoelectric capacitance, ζ_i is the mechanical damping ratio, χ_t is the electromechanical coupling term, and φ_i is the quality normalization characteristic function.

Without damping effect, under short-circuit conditions, the first-order inherent frequency ω_r is expressed as:

$$\omega_1 = \lambda_r^2\sqrt{\frac{YI}{ml^4}} \quad (8)$$

where λ_1 is frequency, Y the elastic module, I is moment of inertia, YI indicates the bending rigidity, and m the mass per unit length.

Determining System Performance

The structure and material parameters of a unimorph beam CPVG with mass are shown in Table 1. The parameters are the same for unimorph and bimorph beams, only the thickness of the unimorph beam is half that of a bimorph beam.

Tungsten is adopted as the mass material with Young modulus 410GPa, Poisson's ratio 0.28 and density 19250kg/m³. The relations between inherent frequency, output voltage and mass are analyzed to determine the system's performance by changing the quality of the mass.

The mode of vibration and inherent frequency of the piezoelectric beam are confirmed by modal analysis (see Figure 2).

Parameter	Piezoelectric layer(PZT-5H)	Substrate (Phosphor bronze)
Density ρ(kg/m^3)	7600	8860
Elastic module Y(GPa)	60.6	110.0
Poisson's ratio μ	0.289	0.330
Piezoelectric constant d_{31}(10^{-12}m/V)	-274	—
Dielectric constant ε_{33}^S(F/m)	1470ε_0	—
Length l(mm)	50	50
Width w(mm)	15	15
Thickness h(mm)	0.4	0.4

Table 1: Structural and material parameters of a unimorph piezoelectric beam

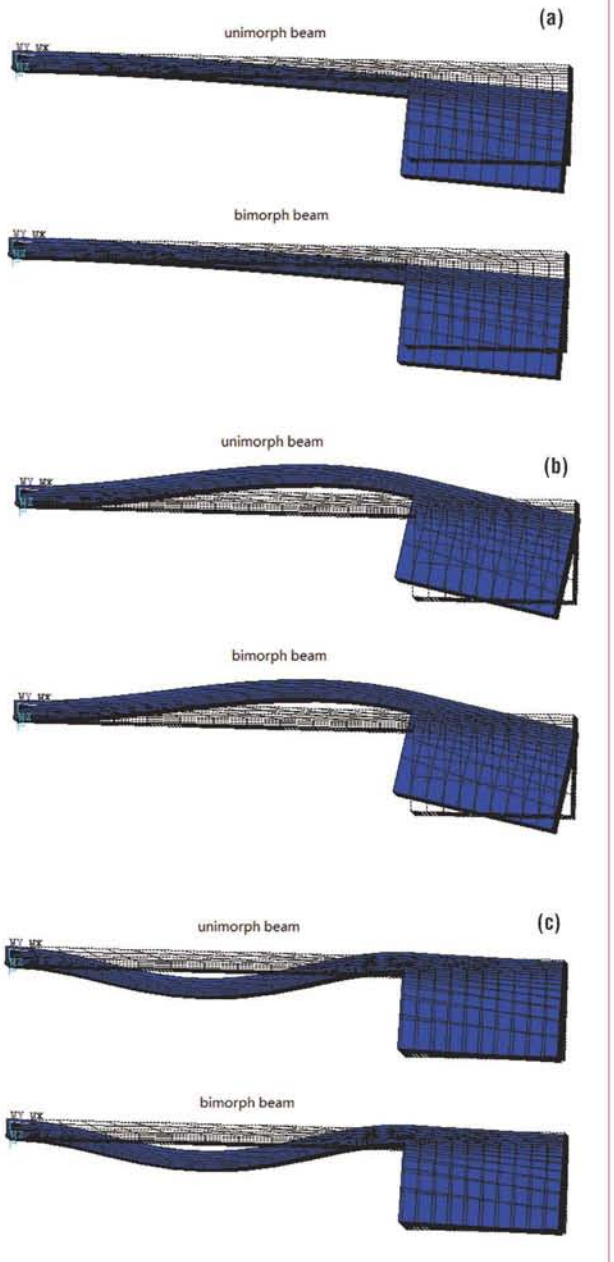

Figure 2: Modal shapes of piezoelectric beam with concentrated mass: (a) First-order modal shape; (b) Second-order modal shape; (c) Third-order modal shape

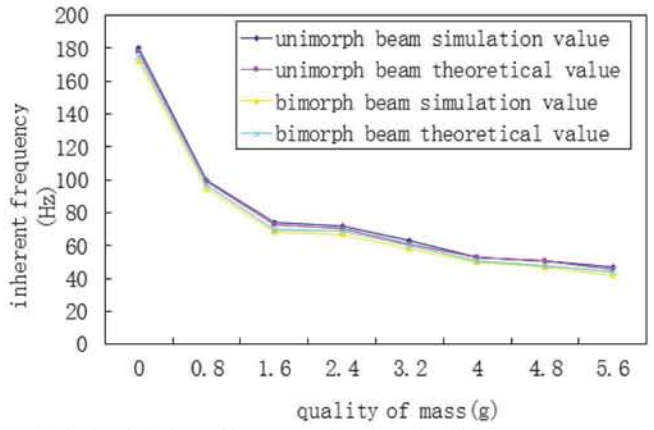

Figure 3: First-order inherent frequency of a piezoelectric beam with concentrated mass

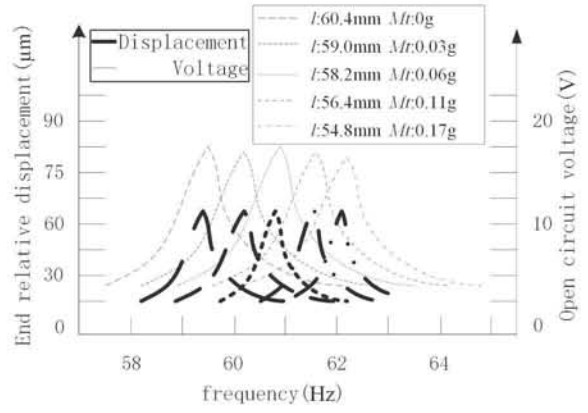

Figure 5: Output voltage and end relative displacement vs frequency of piezoelectric beam with approximate inherent frequency in different configurations

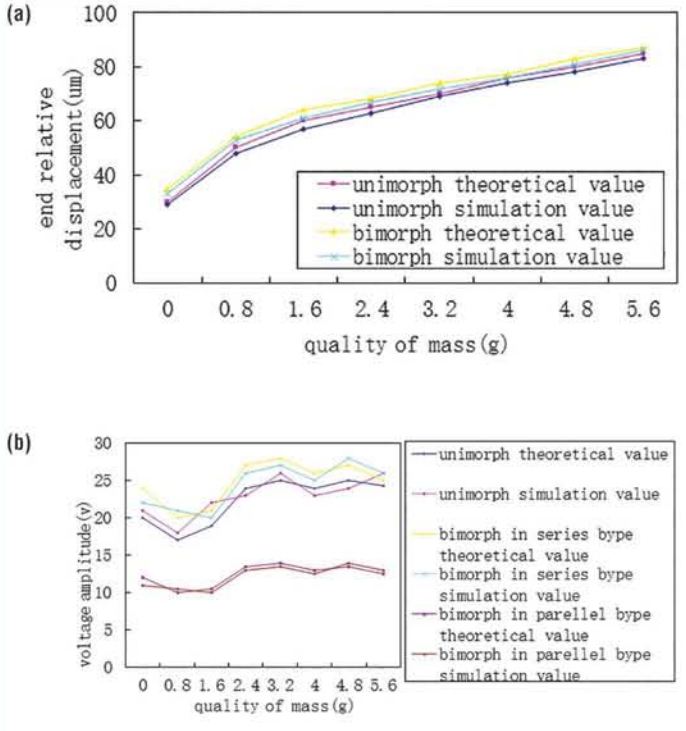

Figure 4: First-order inherent frequency of a piezoelectric beam with concentrated mass: (a) End relative displacement vs quality of mas; (b) Output voltage vs quality of mass

Figure 6: Piezoelectric generator test setup

The first-order inherent frequency of the piezoelectric beam with mass of different characteristics is calculated with Equation 8, with results shown in Figure 3. It can be seen that the simulation results agree with the theoretical values of the piezoelectric beam; the higher the quality of the concentrated mass, the lower the inherent frequency of the piezoelectric beam is. The concentrated stress on the piezoelectric beam increases with the quality of concentrated mass, but excessive concentrated stress can lead to fracture at the roots of the piezoelectric beam. So in practice, the factors of inherent frequency and fatigue strength should be calculated and concentrated mass selected carefully to ensure that bending stress on the piezoelectric beam is within the permissible range.

When ambient excitation changes according to a sine wave, the steady-state response of the CPVG with concentrated mass can be simulated by harmonic response analysis, and the effect of mass quality on the overall performance determined; see Figure 4. Here, the output voltage and end relative displacement of the CPVG are influenced by the quality of the concentrated mass. The end relative displacement rises linearly, but the output voltage doesn't follow, because the concentrated mass leads to larger deformations, increasing the output charge and lowering the inherent frequency.

The relationship between the end relative displacement and output voltage of a bimorph-in-series type beam with different length and mass are studied for the inherent frequency approach. For simulation purposes, the length was chosen as 54.8mm, 56.4mm, 58.2mm, 59mm and 60.4mm, and the

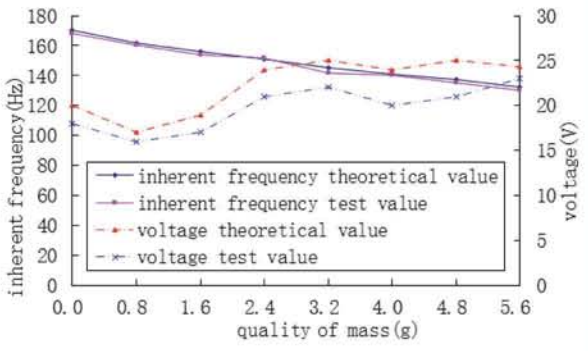

Figure 7: Inherent frequency and maximum open-circuit voltage vs concentrated mass

relevant concentrated mass as 0.17g, 0.11g, 0.06g, 0.03g and zero mass. Results show that the output voltage with the inherent frequency approach and end amplitude are similar, as shown in Figure 5.

Experimental Study

To test the theoretical model, an experimental measurement platform of the unimorph and bimorph beams was created as shown in Figure 6. The equipment includes a GFG-8019G signal generator, GF-10 power amplifier, ZJY-601 vibrostand, BVM-200 vibration meter and DS-1102CD digital storage oscilloscope.

A harmonic excitation signal of tunable frequency is generated using the signal generator, then amplified by the power amplifier to control the vibration of the exciter, and provide the piezoelectric generator with constant excitation. The piezoelectric generator's velocity, accelerated velocity and displacement of fixed support are measured using a vibration meter, and a real-time measurement of the output voltage of the piezoelectric generator is taken with the oscilloscope to calculate the output power for the load resistance.

Figure 7 shows the resonant frequency at maximum open circuit voltage for a unimorph beam 20mm long.

SENSING CHANGE

CONDITION MONITORING IS ESSENTIAL FOR UNDERSTANDING THE HEALTH AND EFFICIENCY OF A MACHINE OR PROCESS. MOREOVER, IF THERE ARE MOTORS, GEARBOXES OR OTHER MOVING PARTS INVOLVED, OF ALL PARAMETERS TO MONITOR, VIBRATION IS ARGUABLY THE MOST USEFUL. **ANDY ANTHONY**, MANAGING DIRECTOR OF MONITRAN, EXPLAINS WHY, WITH EXAMPLES

Within most applications with rotating parts, a change in vibration levels tends to provide the earliest indication that something is wearing or has broken. Also, as vibration is the movement of something, even if it is only air (i.e. noise), energy is being consumed, and if machinery – whether driven by electric motor, combustion engine or a turbine – is vibrating more than it should, then it will consequently be less energy-efficient than intended. In addition, analysis of the vibration signature can reveal the nature of the fault; for example, a broken gear tooth, a worn bearing or a shaft out of alignment.

Vibration Sensors

Vibration sensors are typically based on either piezoelectric or piezoresistive technology. Of these two technologies, the former is more prevalent, and with no moving parts, a vibration sensor offers long-term reliability and stability.

> If considering permanently installing sensors on machinery, it will be important to make optimum use of each sensor's output range, without sacrificing its sensitivity

Figure 1 shows a cutaway of a sensor. A mass is bonded to a piezoelectric crystal which, when placed under tension or compression, generates an electric charge proportional to the acceleration of the mass, the reason vibration sensors are frequently referred to as accelerometers.

The electric charge is conditioned by the circuitry to produce a more useful output; typically DC in the range 4-20mA for ease of integrating the sensor into a monitoring system. However, sensors with AC outputs are also popular.

The output, proportional to acceleration in mm/s/s, may also be conditioned to represent velocity (mm/s) or displacement (mm), and sensors are also available with multiple outputs, e.g. acceleration and velocity. Typical frequency responses range from about 1Hz-10kHz, though some sensors can measure down to DC (0Hz), for applications such as monitoring the movement of large structures such as bridges.

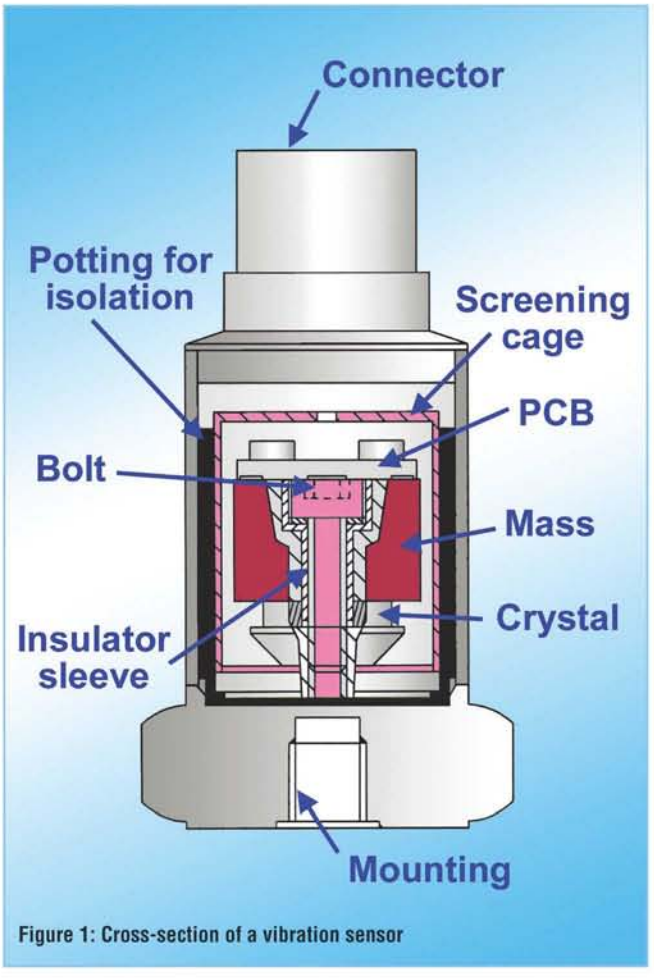

Figure 1: Cross-section of a vibration sensor

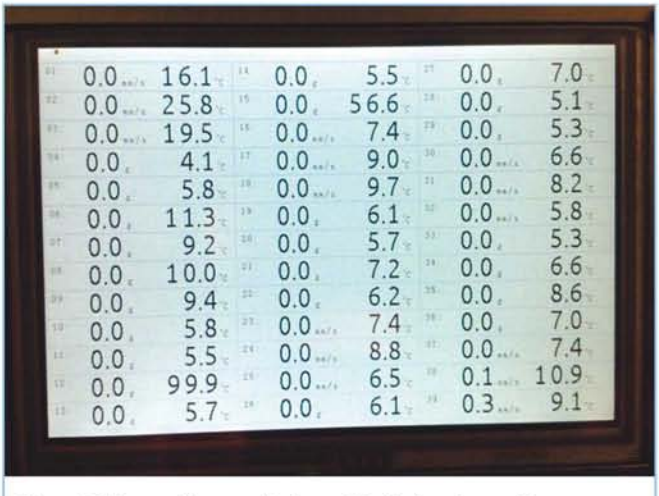

Figure 2: The condition monitoring unit's display shows all 78 channels for 39 dual output sensors

As for operating temperature ranges, even a general purpose sensor will cover -25 to 90°C. For high-temperature applications, sensors are available that can cope with over 200°C.

Best Picture

There are several different types of vibration sensor on the market. If sensors are to be installed as permanent fixtures on machinery, it will be important to make optimum use of each sensor's output range, without sacrificing its sensitivity. Many sensors are guaranteed by their manufacturers to operate across an ±80g range, though they can typically handle far greater forces without fear of damage.

Accordingly, if an AC sensor's sensitivity is 100mV/g, the output will swing between -8V and +8V across its declared operating range. However, if the sensor is likely to be exposed to no more than ±8g then it would be wiser to select one with a sensitivity of 1V/g, as the output voltage swing will provide better resolution of the vibration levels.

As a rule of thumb, it is recommended that any sensor's sensitivity should be such that its output is about 80% of maximum when its machine is operating under normal conditions. As for gauging what 'normal' is, a handheld measurement device such as a vibration meter will help determine not only the levels but also where best to mount the sensors.

With sensors in place, we can begin to use the vibration data. Here it is worth recounting two very different condition monitoring projects, both featuring 24/7 collection of data (see the blue boxes).

Achieving Goals

To monitor the health of a machine or process, in most instances three things must be achieved: (a) determine if levels have changed; (b) the rate at which the levels changed; and (c) automatically raise

EXAMPLE ONE: HAZARDOUS ENVIRONMENT

During construction of a new biomass power station in the north of England, the station's operator identified the need to protect the site's rail load-out system, which is used to transport fuel to the station's burners and which in addition to rail carts includes hoppers, conveyors and feeders. The operator turned to Monitran and engineering reliability specialists Drive Management Services (DMS) to develop a condition monitoring system to interface with the site's Supervisory Control and Data Acquisition (SCADA) system.

In designing the condition monitoring system, the companies determined that multiple assets should be monitored for rises in vibration and temperature levels; and that this could be achieved using 39 dual output sensors. In addition, the station's main handling area is categorised as ATEX zone II, due to the fire and explosion hazards associated with biomass fuel. Accordingly, every aspect of the monitoring system in that area had to be intrinsically safe.

The sensors are permanently mounted on key assets which include motors, gearboxes, fan assemblies and bearing housings. In most cases they are wired into local junction boxes, typically one per asset. Screened multicore cables then connect the junction boxes to a wall-mounted microprocessor-based condition monitoring unit, located in the site's Motor Control Centre (MCC).

The condition monitoring unit was built and pre-calibrated by Monitran and whilst the MCC is not an ATEX II zone, consideration had to be given to the unit being electrically connected to sensors which are in a hazardous environment. Zener barriers were employed, one per channel, to supress any voltages that might cause a spark.

The unit has a 5-inch 800 x 480 pixel LCD screen, which is updated at five-second intervals and displays readings for the 78 channels (see Figure 2); and connection to the site's SCADA is via Modbus TCP Ethernet. The alarm level for each channel was set in the SCADA, on which a 'look-back' history can also be accessed to determine at what rate any of the conditions being monitored might be changing.

Following installation and commissioning of the condition monitoring unit, realistic alarm levels were set in the SCADA; not too high, so that developing faults would go undetected for too long, and not too close to normal operating levels to cause false alarms.

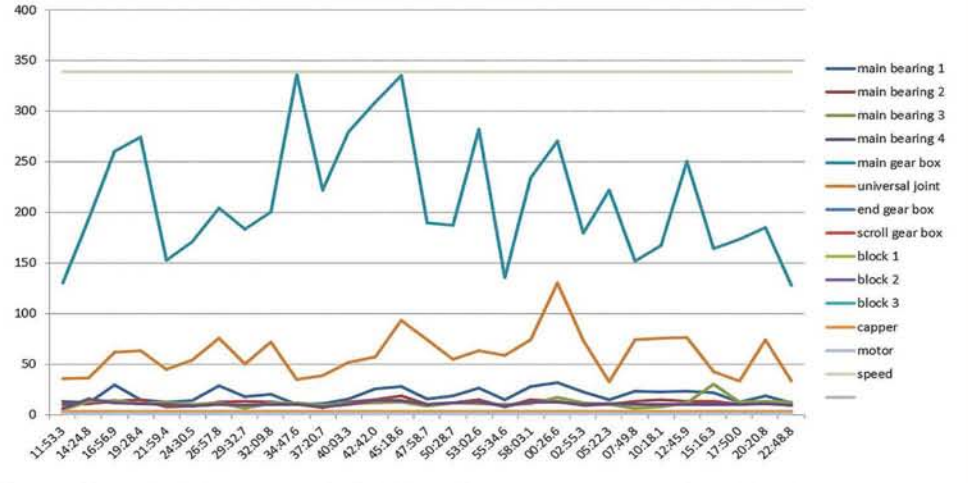

Figure 3: Data collected from one of the Dairyfill machines being monitored. The light blue trace corresponds to vibration levels on the main gear box, which was found to be oscillating on its mount

Figure 4: The Monitran MTN/5000 condition monitoring system

EXAMPLE TWO: THE 'VIRTUAL ENGINEER'

The second example relates to the dairy industry and the bottling of milk. Stork Food & Dairy Systems is a keen advocate of condition monitoring; and condition-based predictive maintenance (CBPM) in particular. The company specialises in the development and support of integrated processing and filling lines for the dairy and other industries. It has 40 Dairyfill rotary fillers in use at UK-based customers.

The fillers typically operate 24/7 and are complex machines, operating at speeds of up to 300 2-litre bottles per minute. Shutdowns other than scheduled maintenance are to be avoided.

In 2009, working with the Institute of Industrial Research (IIR, now known as the Centre for Intelligent Data Solutions), Stork began developing an advanced condition monitoring system called 'Virtual Engineer', for which it received funding under the UK Government's Knowledge Transfer Partnership (KTP).

Monitran made a site visit to see a Dairyfill machine in operation. Based on its observations and experiences from previous projects, it recommended the use of 16 sensors per machine.

Stork's engineers decided to monitor three fillers, fitted the recommended sensors and then used HBM data acquisition units, which can handle up to 16 analogue inputs, to convert the sensors' analogue outputs to 24-bit resolution digital. Data was sampled at a nominal 3kHz and streamed over the Internet to the Centre for Intelligent Data Solutions. With such a high sampling rate it was possible to quickly build a detailed picture of 'normal' behaviour, on a machine-by-machine basis and for different modes of operation.

During the first year of monitoring, anomaly detection algorithms identified six deviations from normal behaviour. Each was investigated and found to be developing conditions which, if left unchecked, would have led to a catastrophic failure. Interestingly, one of the faults was on a machine already protected by a third-party complex spectrum analysis warning system. However, the fault was with a gear which rotates at about 7rpm, a frequency sufficiently low to be masked by the 'noise threshold'.

A further eight conditions have since been detected. Also, Stork's engineers observed some previously unseen spurious vibrations. These turned out to be a fault developing in a height adjustment system, which they had not set out to monitor. The discovery was good news, and it reinforced Stork's conviction that as time goes on and the picture of normal behaviour becomes clearer, any new vibration patterns must be the tell-tale signs of a new fault.

Since the trials, vibration sensors have been fitted to a further eight fillers, which will be monitored using Virtual Engineer. And the ROI? Based on the 14 failures that have been avoided, Stork estimates the savings to be in excess of £2million. Also, Stork believes that Virtual Engineer marks the first use of a remote, real-time, asset monitoring system within a CBPM strategy built primarily around vibration levels and signatures in a dairy application, and possibly within the food and drink industry as a whole.

an alarm if predetermined levels are exceeded. Thankfully, all three goals are achievable with relative ease and well within a typical engineering budget.

Condition monitoring systems, like the Monitran MTN/5000 (Figure 4), are available which are easy to program, in terms of setting data sampling rates, input ranges and resolution, and alarm levels. Once running, they provide a 24/7 'first line of defence'.

The MTN/5000 was launched at the 2014 Southern Manufacturing and Electronics show. It has up to 12 channels and data sampling rates up to 1million/s; input ranges and resolution and alarm levels can be set on a channel-by-channel basis or across all channels.

It works with most sensor types and can also accept voltage or current as input, with raw signals made available at BNC connectors on the front panel. The standard model has 12 digital I/O channels which can be used for multiple alarms or as a communication channel for integration with other systems. As an optional extra, the system can also be fitted with Modbus TCP/IP, for networking purposes or to enable multiple MTN/5000s to operate together within a larger monitoring or control system. ●

IT'S A HARD LIFE

Vibration-based condition monitoring systems are protecting the drive trains of a number of the Indian Coast Guard's hovercraft. Designed by Monitran, the system employs 14 general-purpose constant-current analysis sensors (sealed to IP68) with AC outputs. These feed into a bulkhead-mounted cabinet at which data is made available in different views. The cabinet also feeds a colour-coded status indictor (green for below threshold, red for above) in the cockpit to give the pilot an indication of drivetrain vibration levels.

Wireless Mesh Network. Wired Reliability.

Every Node Can Run on Batteries for >10 Years at >99.999% Reliability

The Dust Networks LTC®5800 and LTP®5900 product families from Linear Technology are embedded wireless sensor networks (WSN) that deliver unmatched ultralow power operation and superior reliability. This ensures flexibility in placing sensors exactly where needed, with low cost "peel and stick" installations. The highly integrated SmartMesh® LTC5800 (system-on-chip) and LTP5900 (PCB module) families are the industry's lowest power IEEE 802.15.4e compliant wireless sensor networking products.

Features

- Routing Nodes Consume <50µA Average Current
- >99.999% Reliability Even in the Most Challenging RF Environments
- Complete Wireless Mesh Solution – No Network Stack Development Required
- Network Management and NIST-Certified Security Capabilities
- Two Standards-Compliant Families: SmartMesh IP (6LoWPAN) and SmartMesh WirelessHART (IEC62591)

Highly Integrated LTC5800 and LTP5900 Families

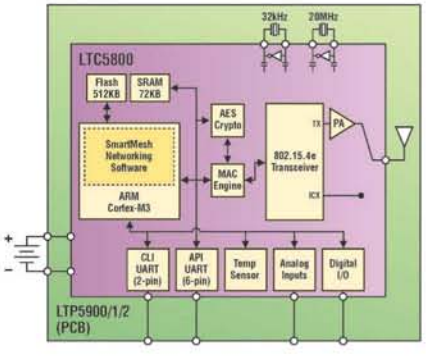

Info and Purchase

www.linear.com/dust

Linear Technology (UK) Ltd.,
3 The Listons, Liston Road,
Marlow, Buckinghamshire,
SL7 1FD, United Kingdom.

Phone: 01628 477066
Fax: 01628 478153
Email: uksales@linear.com

Experience SmartMesh Networks

www.linear.com/starterkits

Arrow Electronics UK Ltd 01279 626777
Farnell 08447 11 11 11

LINEAR TECHNOLOGY

LINEAR EXPRESS
Linear Technology (UK) Ltd. 01628 477066

PRECISE WIRELESS TEMPERATURE SENSOR POWERS ITSELF

KRIS LOKERE, STRATEGIC APPLICATIONS MANAGER FOR SIGNAL CONDITIONING PRODUCTS AT LINEAR TECHNOLOGY, COMBINES HIGH-RESOLUTION TEMPERATURE SENSING, SOLAR-POWERED POWER-MANAGEMENT AND LOW-POWER RADIO FOR WIRELESSLY CONNECTING SENSORS TO A CENTRAL POINT

The Internet of Things refers to a growing trend to connect not only people and computers, but all sorts of systems and devices to the Internet. In applications such as industrial plants or large infrastructure projects, connecting more sensors, or actuators, in more places can increase efficiency, improve safety and enable entirely new business models.

Rather than face the challenge and expense of running cables all around a factory, it is now possible to install reliable, industrial-strength wireless sensors that can operate for years on a small battery, or even harvest energy from sources that are readily available, such as light, vibration or temperature gradients.

Design Overview

This case study shows a real-world design that combines a high-resolution temperature sensor, a power management circuit that uses solar energy when available and battery backup when needed, and a low-power radio module that automatically forms a reliable mesh network to wirelessly connect all sensors to a central point (see Figure 1).

The temperature sensor is based on a thermistor, biased by a low-noise LT6654 voltage reference. The 24-bit delta-sigma ADC LTC2484 reads the thermistor voltage and reports the result via SPI interface. The LTP5901 contains the radio and the networking firmware needed to automatically form an IP-based mesh network. In addition, the LTP5901 has a built-in microprocessor that reads the LTC2484 ADC SPI port and manages power sequencing for the signal chain components.

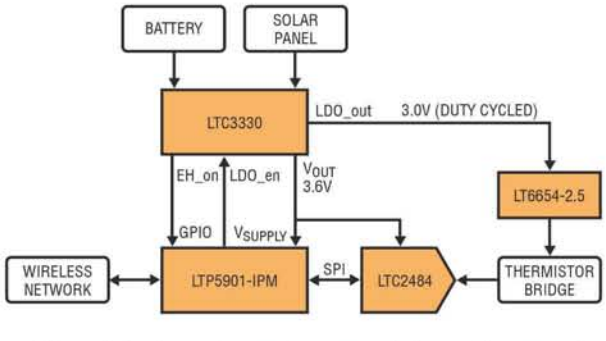

Figure 1: A wireless temperature sensor is formed by connecting a wireless radio module to an ADC, reference and thermistor. The circuit is powered by an energy harvester that can take power from a battery or solar panel

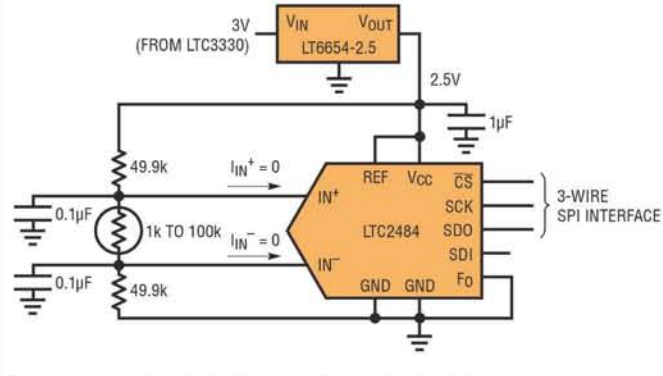

Figure 2: LTC2484 24-bit ADC reads the thermistor voltage. Because the input common-mode voltage remains centred, the Easy Drive ADC draws no input current, which makes for an easy and accurate ratiometric reading

The LTC3330 is a low-power, dual switch-mode power supply (SMPS), powered by a solar panel in bright light conditions, which reverts to a battery to regulate the output voltage. The LTC3330 also includes an LDO used to duty cycle power to the temperature sensor.

The Signal Chain

The design uses a thermistor to measure temperature. Thermistors are well suited to read temperatures in a range well beyond typical ambient temperatures. Thermistors are resistors with a strongly negative temperature coefficient. For example, part number KS502J2 (by US Sensor) is 5k at 25°C and changes from 88k to 875 Ohms over the -30°C to +70°C temperature range.

In this design, the thermistor is connected in series with two accurate 49.9k resistors, and biased by precision voltage reference LT6654 (Figure 2). The LTC2484 delta-sigma ADC

measures the resistor divider ratio with 24-bit resolution. The ADC total unadjusted error is 15ppm, which for this thermistor slope corresponds to a temperature uncertainty of less than 0.05°C. The thermistor is specified with an accuracy of 0.1°C, so that without any calibration the temperature can be measured to that accuracy.

The ADC noise is less than 4μVpp, which corresponds to less than a 0.005°C change in temperature. Therefore, with a calibration step, this system could be used to measure temperature to extremely fine resolution. Since the ADC measures the ratio of thermistor voltage to reference voltage, strictly speaking the reference does not need to be accurate. However, it must be low noise, because variations in reference voltage during the ADC conversion period could produce errors.

The LTC2484 ADC features Linear Technology's Easy Drive input structure. This means that net differential sampling currents during a conversion period are nearly zero. As a result, no measurement errors are induced from input sampling current flowing through the resistive thermistor network, which means no separate op-amp buffer is needed.

Bypass capacitors provide a low impedance path at high frequency. In many cases it is not needed to measure temperature constantly, but rather once per second or even just once per minute. It makes sense to save power during the times that the system does not measure temperature. This application circuit does exactly that, as described below.

Circuit Operation

The resistor network draws up to 25μA from the 2.5V reference. To avoid this power loss between measurements, the power supply to the reference is duty-cycled so it's on only during measurements. The RC time constant at the input of the ADC is about 5ms. By turning on the power 80ms before taking a measurement, full settling at the ADC input is ensured. In fact, since both input nodes turn on at the same slope, readings are accurate well before the theoretical settling time.

The LT6654 is powered from the 3V LDO output of the LTC3330. The LTP5901 microprocessor drives the LDO enable pin of the LTC3330 high and low at the correct times before and after performing a temperature reading.

The LTC2484 automatically enters sleep mode when not converting. The 1μA sleep current is low compared to the already power needs of the wireless radio. Therefore, it is not necessary to duty cycle the power supply to the ADC. By keeping the ADC permanently powered from the same supply voltage as the LTP5901, logic levels at the SPI interface are the same, which helps keep the design simple.

After providing a conversion result through the SPI port, the LTC2484 automatically starts a new conversion and stores the result in its internal register until the user asks to read it again. This can be handy in systems that require temperature to be read very frequently. However, some ultra-low power applications may wait a long time in between readings. To ensure that the

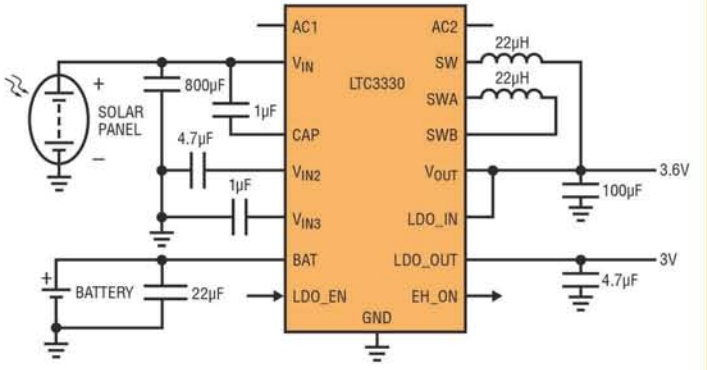

Figure 3: The LTC3330 takes power from the solar panel or battery, automatically prioritizing between the two sources to maintain a regulated output voltage. An additional LDO output is controlled by a logic input pin, which is used to duty-cycle power to the temperature sensor. The LTC3330 generates an output flag to indicate the type of power being used – solar or battery

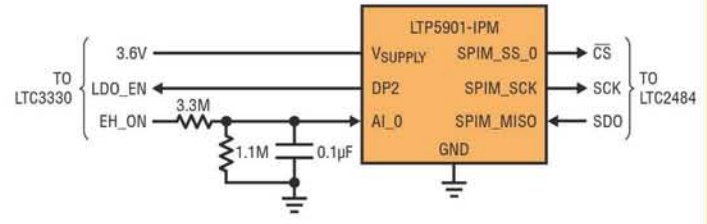

Figure 4: The LTP5901-IPM requires remarkably few connections to run an entire application. All wireless networking functions, including firmware and RF circuitry, are already built in. A 3-wire SPI master talks to the LTC2484 SPI port. A GPIO pin (DP2) controls the power sequencing to the sensor. The built-in ADC acts as a convenient level translator to read the energy-harvesting status flag EH_ON from the LTC3330

temperature communicated to the user is always a fresh reading, this application first toggles the CSb and SCK pins to flush out the 'stale' temperature reading from the ADC register, which automatically starts a new temperature conversion.

The microprocessor waits until the conversion is completed, and then reads the result through the SPI port. Even though a new temperature reading will automatically start again, the system proceeds to shut down the thermistor network (by turning off the LDO) since the result of this extra reading will be subsequently ignored.

The overall power consumption of the temperature sensor circuitry can be estimated as follows. First, sum the current of the reference (350μA), thermistor network (25μA) and ADC (160μA when converting) for a total of 535μA (see Table 1). Then, consider how long this current will be on. The ADC takes about 140ms for a conversion, and prior to that we wait 80ms for the reference and thermistors to settle. Add in some time for the SPI readout and we are at about 300ms.

To consume a current of 535µA during 300ms corresponds to a charge of 160µC. We should add to this the charge needed to charge up the 4.7µF supply bypass capacitor to the voltage reference, because this node gets recharged from 0V to 3V with every reading. This 14µC charge brings the total to 174µC per temperature reading. If we take one temperature reading every 10s, this works out to an average current consumption of 17µA. Other examples of average supply current are given in Table 2.

LT6654 Reference	350µA
Thermistor Network	25µA
LTC2484 ADC	160µA
Total	535µA

Table 1: Signal chain current consumption (when active)

Temperature Read Frequency	Average Current
Once per second	170µA
Once per 10 seconds	17µA
Once per minute	2.9µA

Table 2: Average signal chain current consumption based on read-frequency power management

Power Management

The LTC3330 manages all the power for this application. It includes two SMPSs and one linear regulator in a small monolithic package. A buck-boost converter can take power from the battery to maintain a regulated output voltage (set to 3.6V for this application).

A separate buck converter can also take power from the solar panel to regulate the output voltage to the same level. An internal prioritizer ensures that solar power is used when possible, and only draws power from the battery when needed (see Figure 3).

For other applications, the LTC3330 also supports AC energy-harvesting sources, such as piezo crystals which generate an AC voltage proportional to vibrational energy (check out the article on piezoelectric vibration generation, also in this issue).

The LTC3330 draws less than 1µA quiescent current, making it suitable for this low-power wireless application. The loss in the power supply is only a small fraction of the total power loss, so most of the power is available for the load, the temperature sensor and wireless network.

In addition to the two switch-mode power supplies, the LTC3330 includes an LDO with a separate LDO enable pin. This feature is handy for these duty-cycled applications. The voltage reference and thermistor network are powered from the LDO. This not only reduces switching noise, but also allows the application to toggle power to the signal chain on and off, whilst keeping power to the wireless radio always on. Even though the wireless radio does not consume much power between transmissions, it is essential that it always remain biased up to keep timers running correctly and the entire network time-synchronized. The microprocessor inside the wireless radio sequences the LDO enable pin at the correct times to prepare the signal chain for a temperature reading.

The LTC3330 provides an output flag (EH_on) which tells the system whether power is being drawn from the battery or from the solar panel. It can be informative for the end user to have real-time access to this information. Therefore, we let the microprocessor inside the wireless radio read this output flag and transmit it through the network, along with the temperature data itself. The logic level for this EH_on output is referred to an internal bias voltage of the LTC3330, which varies depending on the operating mode and can be higher than 4V.

Rather than connecting that output pin directly to the lower-voltage logic input of the wireless radio, we divide it down and feed it into a built-in 10-bit ADC that is part of the microprocessor. In this case, we just use that ADC as a comparator to indicate which power source the LTC3330 is using.

Wireless Networking

The LTP5901 is a complete wireless radio module, which includes the radio transceiver, embedded microprocessor and networking software. The physical format is that of a small printed circuit board, which can be easily soldered onto the main circuit board that contains the rest of the application (signal chain and power management).

The LTP5901 performs two functions in this application: wireless networking and housekeeping microprocessor (Figure 4). When multiple nodes of LTP5901 are powered up in the vicinity of a network manager, the nodes automatically recognize each other and begin forming a wireless mesh network. The entire network is automatically time-synchronized, which means that each radio is powered on only for very short, specific time intervals. As a result, each node can function not only as a source of sensor information, but also as a routing node to relay data from other nodes toward the manager. This creates a highly reliable, low-power mesh network, where multiple paths are available from each node to the manager, even though all nodes – including the routing nodes – operate on very low power. A typical range for this radio technology is 100m between nodes, with even longer range possible in favourable outdoor conditions.

The LTP5901 includes an ARM Cortex-M3 microprocessor core, which runs the networking software. In addition, this core can be programmed through user-supplied firmware to perform tasks specific to the user application. As a result, many applications can be built without needing any third-party microprocessors.

In this example, the microprocessor inside the LTP5901 manages the power sequencing to the temperature sensor by turning the LDO of the LTC3330 on and off at the correct times, so as to conserve power between temperature readings. The LTP5901 communicates directly to the SPI port of the 24-bit ADC

that reads the temperature sensor. Finally, the LTP5901 reads the power status output flag (EH_on) from the LTC3330, which indicates whether solar light or the battery is used to power the circuit.

Power consumption of the wireless radio can be estimated using the online SmartMesh Power and Performance Estimator tool on Linear Technology's website at www.linear.com/products/smartmesh_ip. For a typical network of 20 motes, where 10 motes have a direct wireless connection (1-hop) and 10 others have an indirect connection to the manager (2-hop), average power consumption is about 20µA for the 2-hop nodes and 40µA for the 1-hop nodes. These figures are for each node reporting temperature once per 10 seconds.

The reason 1-hop nodes consume about twice as much power is because they transmit not only their own sensor data, but also act as routing nodes to forward the sensor data from some of the 2-hop nodes.

The power levels mentioned here can be further reduced by about a factor of two if a feature called "advertising" is turned off. Once advertising is turned off, the network will no longer recognize new nodes that want to join it. Other than that, there is no impact on network operation.

Overall Power Consumption

Total power consumption of the complete application circuit depends on various factors, including how often each sensor measures temperature and how the nodes are configured in the network.

Typical power consumption for a sensor node reporting once per 10 seconds is less than 20µA for the sensor portion and can be 20µA for the wireless radio, for a total average load current of about 40µA.

A small 2-inch x 2-inch solar panel (for example, the Amorton series) can generate 40µA under even relatively moderate indoor lighting conditions (200 lux), and much more in bright light. This means that this application could run entirely on power from the solar panel in many conditions.

If the circuit is in the dark and needs to run entirely on battery power, an ordinary 2.4Ah AA battery (such as the Tadiran XOL series) could power this application for almost seven years. In low or variable light conditions, the circuit automatically toggles back and forth between solar power and battery power, so any available solar power is used to extend battery life.

SOFTWARE DEFINED RADIO MEETS DEMANDING APPLICATIONS

HAVING REACHED MATURITY, THE WORLD OF COMMUNICATIONS TECHNOLOGY IS BEING TURNED UPSIDE DOWN BY THE RAPID ADVANCEMENT OF SOFTWARE DEFINED RADIO. **BRANDON MALATEST**, FOUNDER OF PER VICES, WHICH DEVELOPS COMPLETE WIRELESS SYSTEMS, EXPLAINS

Software Defined Radio (SDR) has had the attention of every serious player in the RF market for some time. The ease of design and total versatility of SDR has captured the attention of a new generation of both RF and digital designers, and opened up new horizons of performance. SDR has already proven to be a cost-effective platform with specifications that challenge conventional technologies, while providing for future upgrades that adapt to unforeseen and unusual technology developments.

The concept of SDR has been around since the 1970s, but practical uses were significantly limited by period technology, especially in the areas of RF amplifiers, tuners and digital processing. Recent advances in semiconductor processing, wide-band analog components and digital converter technology have led directly to more widespread use of SDR in ever more demanding applications.

Performance

Most software defined radios share a similar architecture: an antenna connects to a radio front-end that interfaces to a digital signal processing (DSP) system (see Figure 1). The digital system may consist of a single, fixed-purpose component, or a generalized system that includes discrete converters (ADCs and DACs) interfacing to an FPGA or other processing device.

Performance is generally judged on a number of key specifications, including: tuning range, sampling bandwidth, number of independent channels, clock stability and processing power for backhaul technology, among others.

The individual components dictate the frequency range in which the transceiver can operate. This can range from a few kHz through to hundreds of GHz, depending on the application.

RF bandwidth is another driving factor in most SDR choices. This is the amount of spectrum able to be captured instantaneously. Greater bandwidth allows more information to be captured and higher data throughput rates to be obtained.

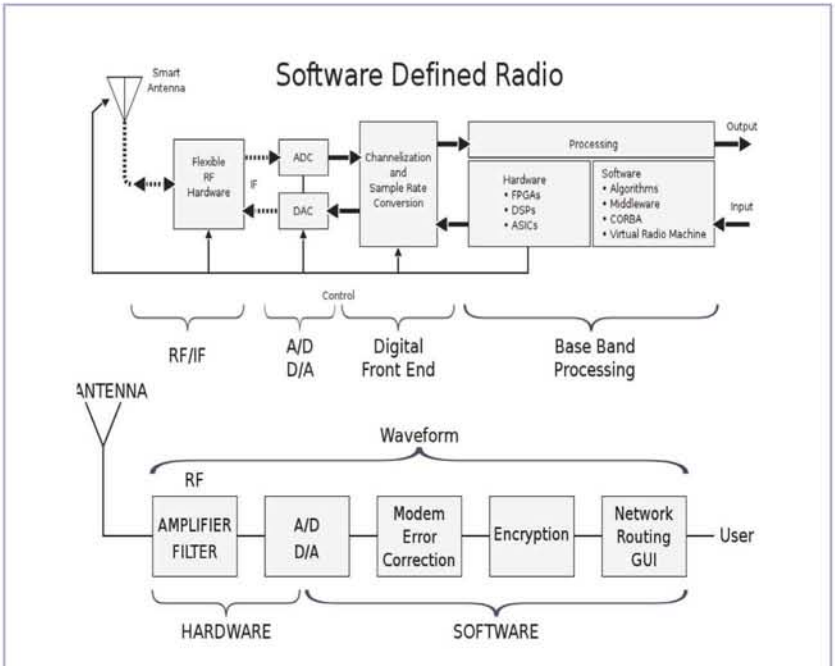

Figure 1: SDR scheme

Why has this become important? 4G cell services have channel widths ranging from 1.4-20MHz, and use spectrum between 700 and 2600MHz. A high-end 4G system needs to cover this range quickly and efficiently, and SDR fits the need perfectly. Similarly, a military spread-spectrum secure communications system requires great agility to deliver security and adapt to local conditions. SDR, when paired with the appropriate processing power, presents a perfect solution.

Conventional radios are simple systems, built for operation using a small part of the spectrum and typically only one chain. Most radios receive on one frequency and transmit on another, sometimes in full-duplex, sending and receiving concurrently, but often only half-duplex; able to send or receive at any given time,

> The concept of SDR has been around since the 1970s, but practical uses were significantly limited by period technology, especially in the areas of RF amplifiers, tuners and digital processing

but not both concurrently. SDR simplifies building a multi-channel radio in which sending and receiving in different parts of the spectrum is required. In an SDR receiver, the post front-end stages of amplification, mixing and demodulation are digital, requiring only software to define the application. In an SDR transmitter, the signal is generated digitally (again, defined in software alone) and applied directly to the RF amplifiers, eliminating analog signal generation stages.

With less time spent aligning and tuning analog hardware, the radio can be fitted with multiple independent receive and transmit hardware. Quality, reliability and cost are improved by reducing the tunable parts count, and the overall functionality of the finished product may be multiplied by the number of available channels.

Specification	min	nom	max	units
Temperature				
Card Operating Temperature		70		C
Analogue				
RF Tuning (HMC833)	25		6000	MHz
Dyn. Range (RX,TX)	10		70	dB
SFDR (RX, TX)			65	dB
Power Gain (RX, High) @2GHz	-4.5		65	dB
Power Gain (RX, Low) @ 125MHz	-15		+55	dB
Nominal RF Input Power		-20		dBm
Rx, Noise Figure	3.5		11	dB
TX Power @ 10MHz		20		dBm
Digital				
FPGA - Arria V ST SOC		5ASTMD3E3F31		-
10Gbe Data Rate (full duplex)		8		Gbps
ADC resolution		16		bits
ADC Sample Rate (per IQ Channel)		322.265625		MSPS
DAC resolution		16		bits
DAC Sample Rate (per IQ Channel)		322.265625		MSPS
Decimation (2^n), n=[0,5]	0		32	-
Interpolation (2^n), n=[0,5]	0		32	-
Internal Reference (10 MHz)				
Frequency Calibration (20°C)	-5		5	ppb

Figure 2: Crimson's observed performance. These specifications reference observations taken during internal use and development

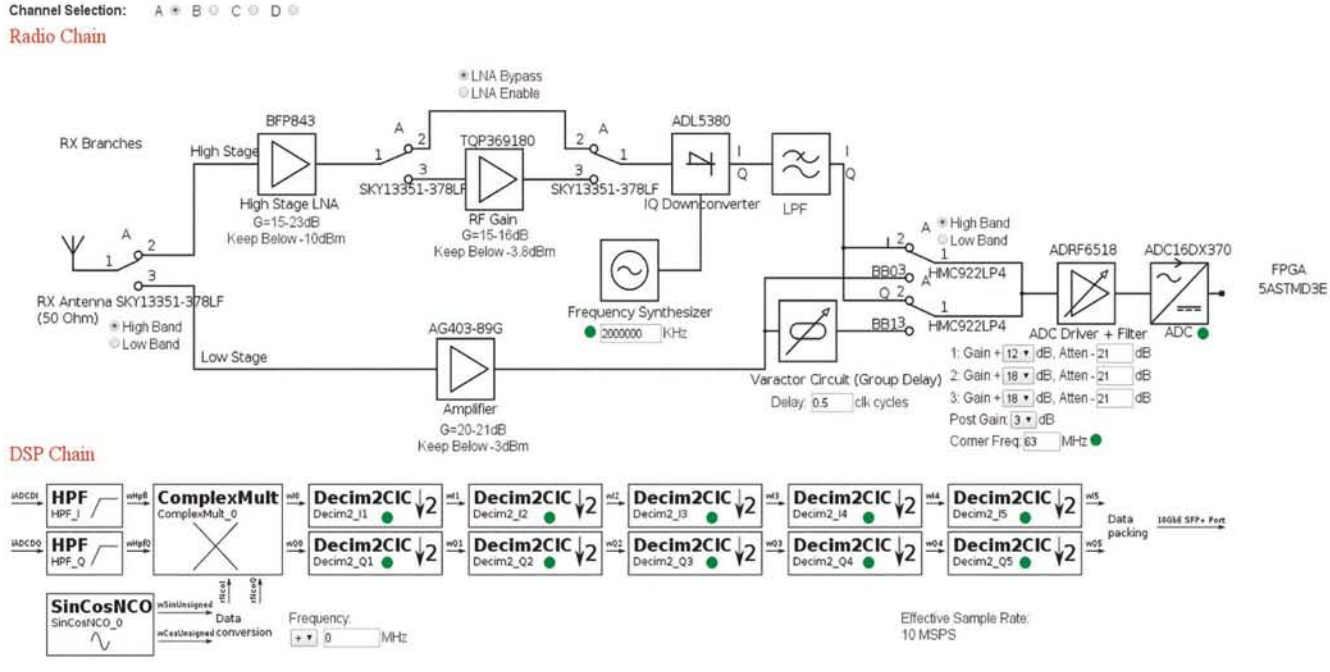

Figure 3: Per Vices's Crimson web interface

PER VICES'S CRIMSON SOLUTION

Among the best products on the market, the Per Vices Crimson has an operating frequency range from DC-6GHz and over 1200MHz of RF bandwidth across four fully-independent Rx and Tx channels. It has a high-stability 10MHz clock (±5ppb) which allows all components to be synchronized precisely.

On the digital end, Crimson offers dual SFP+ connectors for high transfer rates (up to 20Gbps total throughput) and low latency for uses where data is streamed to another unit. With that in mind, Crimson also offers a powerful FPGA (Altera's Arria V ST) with an on-board dual-core ARM Cortex-A9 processor (see Figure 2).

By using a high-stability clocking network with very low phase-noise, Crimson is able to meet the requirements associated with the most demanding applications, including LTE basestations and radar applications. Its 1200MHz instantaneous RF bandwidth allows it to be used as a spread-spectrum transceiver or data aggregator with the dual SFP+ connectors enabling high-speed data transfer rates of up to 20Gbps.

Crimson also provides a number of configuration interfaces, including a web-based SCADA-like interface that allows users to graphically configure the entire DSP chain. By using a web-based control structure, the unit can be viewed and controlled from a remote location. In addition, Crimson provides a full command line interface and an API for system integration (see Figure 3).

There are a few qualities of SDR that have become cutting edge, and Crimson's very high RF bandwidth and powerful onboard processor are key. The user can create non-standard or proprietary techniques by simply programming them into the DSP chain on the FPGA, or create programs to run on a SoC. New modulation modes can easily be adapted in the future.

Software requires less bench-time to design and prototype than hardware, thus the time to market is much shorter with SDR. This can translate to unique market advantages for the agile competitor, since a single product can be used for many different dedicated functions by changing its firmware. This allows many OEMs to use a single, high-quality SDR, with each company selling completely different radio and processing functions.

Agile Radio Hardware

A stable clock is needed to ensure that each of the components in the hardware shares a common time base for operation. Clock stability minimizes undesirable effects such as phase shift, frequency drift and jitter. A noisy clock will reduce overall system performance by degrading the signal processing components and nullifying any advantage gained in a low-noise RF front-end. A clean, stable, jitter-free clock allows LTE basestations, GPS receivers, radar and satcomm data streams to work at peak performance.

Some SDRs on the market have a backhaul feature for the digital information to be passed to another system for processing. Connectivity can come in many forms, such as USB, Ethernet, PCIe and others. Typically, two features are considered when determining backhaul requirements: data transfer rate and latency. The data transfer rate will define how quickly data can pass from the SDR to another system. The faster the data rate, the more data that can be transferred at any given time. Latency is the time delay between sent and received information. The greater the latency, the greater the time required for information from the SDR to reach the external system.

Other SDRs offer on-board processors and/or field programmable gate arrays (FPGAs) for digital signal processing. These allow for quick mathematical operations on a digitized signal, transforming it into information that can be used directly as audio/display output of the radio, or passed on to other resources for more sophisticated processing and analysis.

An SDR design with wide bandwidth and broad frequency range, a stable clock and processing power that supports backhaul operations allows the designer to produce uniquely agile radios, capable of quickly adapting equally well to the changing conditions of the market or the battlefield.

Applications

In the case of military and government applications, SDR transitions long-term maintenance from a component-based after-market supply system to one where the hardware is a quality choice based on technology available at the time, and software provides functional continuity to the original equipment. Older SDR systems can be maintained, not by repairing individual components, but by replacing hardware with current technology and supplying software that conforms to the original specs.

High-quality equipment with internal redundancy and large bandwidths will reap the benefits of this change. Resilience and flexibility are sought after in mission-critical applications. SDR provides the ultimate in a generalized radio platform: hardware (multiple receive/transmit paths), software (multiple software controllers) and style (multiple communication methods). A communications project could, for example, use satcomm, HF/VHF and standard 4G technology for the high-reliability communications and a UHF control channel or TCP/IP for management functions. This complete application could be hosted in a 1U form-factor, using Per Vices's Crimson, for example.

SDR is now being used in the test and measurement market, broadcast radio and TV, mobile communications, cable systems and even by amateur radio operators. SDR has long promised and now delivers a giant leap forward in value. The introduction of SDR equipment with high-performance processing and large bandwidths provides a turning point in a market that is about to transition from its traditional manufacturing model.

The future belongs to the ones who can grasp the importance of this change and bring new system designs to the market. It will be no surprise when many other markets start to move toward software defined radios for all of their wireless needs. ●

AC-DC Battery Backed Power System 1U 19" Rack Mounting up to 300 Watts

The PFD Series is a no break system to provide constant DC power without interruption in the event of an AC mains failure. Available in 150W and 300W versions and nominal DC outputs of 12V, 24V or 48V

FRONT VIEW

REAR VIEW

Features

- AC Input 180-264VAC 50/60Hz
- Nominal 12V, 24V or 48V DC output versions
- With external batteries can provide constant power without interruption
- Can power your load and charge batteries simultaneously
- Zero interruption in the event of AC power failure
- Intelligent battery condition monitoring with low battery voltage shutdown
- Full protection for over load, short circuit, over voltage and over temperature
- Front panel LED display monitoring
- Dry contacts, RS232, USB and optional SNMP output monitoring
- Temperature controlled fan

POWER SOLVE

www.powersolve.co.uk

Tel: 44-(0)1635-521858 Email: sales@powersolve.co.uk

SENSORS IN WIRELESS WEATHER FORECASTING APPLICATIONS

IN THIS SERIES, **PROFESSOR DOGAN IBRAHIM** OF THE NEAR EAST UNIVERSITY IN CYPRUS PRESENTS DIFFERENT TYPES OF RF SYSTEMS FOR EMBEDDED APPLICATIONS. HERE, HE DISCUSSES WIND SPEED AND DIRECTION SENSORS AND PRESENTS A MICROCONTROLLER-BASED SYSTEM USING OFF-THE-SHELF COMPONENTS

Wind speed and wind direction are important parameters in weather forecasting, and especially in aviation. Anemometers measure wind speed and they are among the most common weather station equipment.

The anemometer has changed little since its invention in the 15th century. Nowadays there are several types, some mechanical and others electronic. In a mechanical anemometer the rotation mechanism's speed is proportional to the wind speed, so wind speed can be calculated with great accuracy.

The three-cup anemometer, where the axis of rotation is vertical, is probably the oldest known mechanical anemometer. Such anemometers respond quickly to sudden wind changes and are widely used.

Vane-type anemometers are also mechanical devices, but they look like windmills, where the axis of rotation is horizontal and parallel to the direction of the wind. Since the direction of the wind changes, it is necessary to change and align its horizontal axis to the direction of wind. A tail is usually employed to rotate the anemometer in the direction of the wind.

The wind direction in mechanical anemometers is easily measured using a calibrated tail with, for example, magnetic sensors (e.g. Hall Effect sensors). As the tail rotates, a voltage is obtained based on the orientation of a magnet, with the output voltage proportional to the direction of the tail.

In electronic anemometers there are no moving parts, so they are not affected by dust or mechanical aging.

The hot-wire anemometer is a commonly used electronic anemometer, with a working principle based on the change of electrical resistance with temperature. Here, a very fine wire is electrically heated to a temperature above the ambient. Air flowing over the wire has a cooling effect on it, changing its resistance. Thus, by calculating the wire resistance from knowing the output voltage, the air flow is easily determined and hence the wind speed. Because of their high accuracy, hot-wire anemometers are used in research and to study air dynamics and related subjects.

Sonic anemometers use ultrasonic sound waves to measure wind velocity, measuring the time it takes for the sound waves to travel between the transducers. Because of their no-moving-parts and reliability features, these anemometers are used where traditional mechanical devices cannot be. Two-dimensional sonic anemometers have four sensor arms and are used to sense wind direction as well as speed.

Acoustic resonance anemometers are a variant of sonic anemometers, where an array of ultrasonic transducers is built into a cavity. As wind passes through the cavity, phase shift is measured by each transducer, and the wind speed and direction can be determined.

In this article, the Vortex (www.inspeed.com) cup-based wind speed sensor and the e-vane wind direction sensor hardware are used in a microcontroller-based project. Both, wind speed and wind direction data, are sent to a receiving station using a commercially-available radio modem, where once received they are processed and displayed.

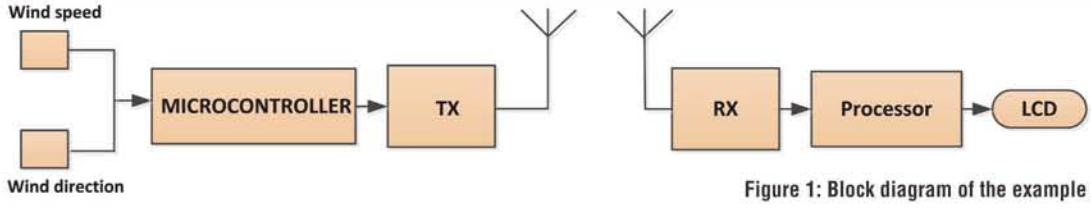

Figure 1: Block diagram of the example system

Example System

Figure 1 shows the block diagram of a basic telemetry system measuring wind speed and direction. Here, the transmitting side consists of the Vortex rotating cup wind sensor (Figure 2), the e-vane wind direction sensor (Figure 3), the Start USB for PIC development kit (www.mikroe.com) and a transmitting modem module.

The Start USB for PIC kit is a PIC-microcontroller-based development board with the PIC18F2550 microcontroller, operating with an 8MHz crystal. The microcontroller can be programmed via the mini USB port. The microcontroller is shipped pre-loaded with a Bootloader program so it can be directly programmed from a PC. The development board provides access to the microcontroller I/O pins through board-edge connectors.

The receiving side consists of a receiving modem, a processor and a display. In practice the processor could be a microcontroller, a PC, the Raspberry Pi, or any other digital computer.

Wind Speed

The Vortex wind speed sensor is a 3-cup mechanical sensor that can measure speeds to over 125mph. A reed switch/magnet in the rotating arm provides one pulse per rotation, which helps calculate wind speed. The sensor operates at 2.5mph per Hz (2.5mph per pulse/s).

There are basically two methods to calculate wind speed: In the first method, time between two adjacent pulses is measured, for example, by using the microcontroller's timer module. If this time is, say, T milliseconds, then the wind speed is given by:

$$\textbf{Wind speed (mph)} = 2500/T \quad (1)$$

In the second method, the pulses are counted during a given time interval. The wind speed is then calculated from:

$$\textbf{Wind speed (mph)} = 2.5 \times (P/t) \quad (2)$$

where P is the number of pulses in the interval, and t is the interval in seconds.

In this article the second method is used and the time interval is taken to be 10s in order to get accurate results. The pulses in this interval are counted using the microcontroller's timer module, where they provide clock to the timer. The wind speed is then calculated as:

$$\textbf{Wind speed (mph)} = 0.25 \times P \quad (3)$$

The calculated speed can be converted into m/s by multiplying it by 0.44704.

Figure 2: Vortex wind speed sensor

Figure 3: e-vane wind direction sensor

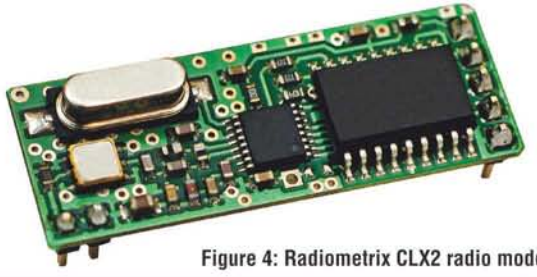

Figure 4: Radiometrix CLX2 radio modem

Wind Direction

The e-vane wind direction sensor is a mechanical vane that rotates freely with the flow of air. The sensor is equipped with a precision Hall Effect sensor and is operated by a +5V external voltage. It produces an analog output voltage based on the orientation of a magnet attached to the vane shaft. The sensor is calibrated with true North corresponding to 0V. Thus, by measuring the output voltage we can find the actual wind direction. In this article the sensor voltage is measured using the microcontroller's ADC converter channel.

The Modem Pair

The Radiometrix CLX2 radio modem (Figure 4) is used in this project to transmit wind speed and direction data to the receiving station. This is a 19200-baud half-duplex serial UHF modem operating in the license-exempt European 433.05-434.79MHz band. The modem module operates from a +3.3V supply; its use is extremely simple, requiring an external 50Ω antenna and that its TXD pin is connected to the UART output pin of the microcontroller. CLX2 provides 2mW output power and consumes only 23mA current whilst transmitting data.

The receiver side also uses a CLX2 modem in receive mode. The receiver has a sensitivity of -95dBm and consumes 13mA of current. The RXD pin of the modem is connected to the UART input of the microcontroller to capture the received data.

Figure 5 shows the circuit diagram of the transmitter hardware (the receiver hardware is not shown due to its complexity; it also depends on the type of processor used). The wind sensor is

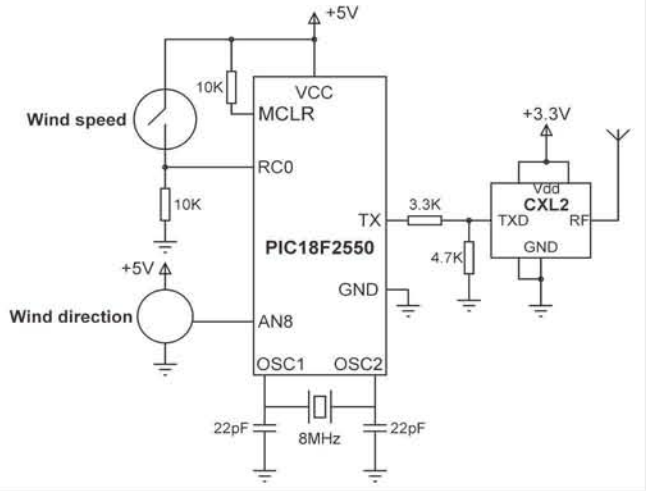

Figure 5: Circuit diagram of the transmitter hardware

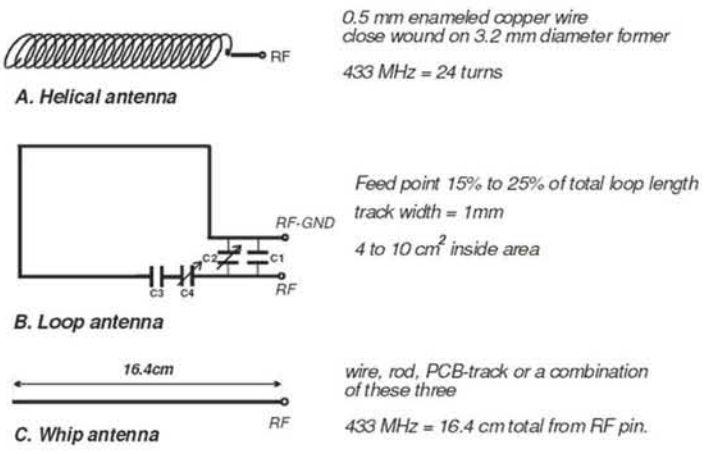

Figure 9: Antenna types in radio telemetry applications

```
BEGIN
        Configure microcontroller I/O ports
        Configure UART
        Configure Timer
        DO FOREVER
                Read wind direction from ADC channel 8
                Calculate wind direction
                Read number of pulses in 10 seconds
                Calculate wind speed in mph
                Send wind speed and direction to UART transmit buffer
                Wait 1 minute
        ENDDO
END
```

Figure 6: Operation of the transmitter program

```
BEGIN
        Configure I/O ports
        Configure UART
        Initialize LCD
        DO FOREVER
                Read wind speed from CXL2 modem
                Read wind direction from CXL2 modem
                Display wind speed and wind direction on LCD
                ENDIF
        ENDDO
END
```

Figure 7: Operation of the receiver program

connected to digital input RC0 of the microcontroller through a 10K pull-down resistor. Thus, as the sensor rotates, a digital signal is sent to pin RC0 once per revolution. The output pin of the e-vane direction sensor is connected to analog input AN8 (channel 8) of the microcontroller. The ADC has a 10-bit (1024 quantization levels) resolution and operates from a +5V supply.

The Software

Software for the test system is based on the mikroC Pro for PIC language. Figure 6 shows the transmitter program's operation, which executes an endless loop. The program reads the wind data from the sensors every minute and sends it to the CLX2 transmitting modem in serial format using the mikroC's built-in UART functions.

Operation of the receiver program is shown in Figure 7. The program operates in an endless loop; the wind speed and wind direction data are received via the CXL2 receiver modem and displayed on an LCD.

The entire microcontroller transmitter program listing is shown in Figure 8 (again, the receiver software is not shown due to its complexity and since it also depends on the type of processor used). At the beginning of the main program, the wind speed sensor and wind direction sensor port pins are configured as inputs and the UART is configured to operate at 19200 baud. The program then configures TMR0 to generate interrupts every second. TMR1 is also configured to count from the pulses generated by the wind speed sensor hardware. The rest of the program executes an endless loop where the wind speed and direction are sensed and sent to the radio modem through the UART. Function Read_Wind_Direction() reads the wind direction from the analog port and converts it into degrees. Similarly, function Read_Wind_Speed() reads the wind speed and converts it into miles per hour.

The Antenna

The type of antenna used in radio telemetry applications depends on several factors, including frequency, power, range, environment and whether the stations are fixed or mobile.

In short-distance UHF applications three types of antenna are recommended by Radiometrix (Figure 9): whip, helical and loop. The whip antenna is a ¼-wave wire rod, or PCB track, connected directly to the RF pin of the TX/RX module. Optimum length is 16.4cm @ 433MHz. The open circuit (hot) end should be kept well away from metal components. Whip antennas give good performance, but their size can be large in VHF applications.

The helical antenna is a wire coil made of 0.5mm enamelled copper wire close wound on a 3.2mm diameter former, 24 turns @ 433MHz. This is a very efficient high-Q antenna, small in size.

The loop antenna is usually made from 1mm-width PCB track and is tuned by a fixed or variable capacitor. It has high immunity to proximity detuning.

In long-distance radio telemetry applications, it is common to use directional antennas (e.g. Yagi, or sectorial antennas). At lower frequencies (e.g. VHF or HF) it is common to use fixed antennas because of their large size. ●

```
sbit Wind_Speed_Data at RC0_bit;
sbit Wind_Speed_Dir at TRISC0_bit;
sbit Wind_Direction_Dir at TRISB2_bit;

unsigned char mphTxt[16], WindDirTxt[16], MQ7_Available = 0;
unsigned char WindSpeedAvailable, StartTimeer1, Timer1secs, Start_Timer1 = 0;
unsigned long Vin;
unsigned int seconds = 0;

void Read_Wind_Direction()
{
        float Degrees, V;
        Vin = ADC_Read(8);                                  // Read wind direction
        V = ((float)Vin*5.0 / 1024.0);                      // Convert to Volts
        Degrees = V*360.0/5.0;                              // Wind direction in degrees
        floatToStr(Degrees, WindDirTxt);                    // Convert to string
}

void Read_Wind_Speed()
{
        unsigned char Clow, Chigh;
        float Pulses, mph;
        unsigned int Count;
        WindSpeedAvailable = 0;
        Timer1secs = 0;
        TMR1H = 0;
        TMR1L = 0;                          // Load Timer 1 with 0000H
        Start_Timer1 = 1;                   // Start Timer1 for 10 seconds
        while(!WindSpeedAvailable);                 // Wait until available
        Clow = TMR1L;                                       // Wind speed count LOW byte
        Chigh = TMR1H;                                      // Wind speed count HIGH byte
        Count = (unsigned int)Chigh*256 + Clow;             // Total wind speed count
        mph = (float)Count / 10.0;                  // Count in 1 second
        mph = 2.5*mph;                                      // Convert to mph
        FloatToStr(mph, mphTxt);                    // Convert to string
}
void interrupt()
{
        TMR0H = 0x48;
        TMR0L = 0xD2;                       // Reload TMR0
        if(Start_Timer1 == 1)
        {
                T1CON.TMR1ON = 1;           // Start Timer 1
                Timer1secs++;
                if(Timer1secs == 10)
                {
                        T1CON.TMR1ON = 0;       // Stop Timer1
                        WindSpeedAvailable = 1; // Set speed available flag
                        Start_Timer1 = 0;
                }
        }
        INTCON.TMR0IF = 0;                  // Clear TMR0 interrupt flag
}

void main()
{
        ADCON1=0x06;                                        // Configure I/O ports
        UART1_Init(19200);                                  // Initialize UART
        Wind_Speed_Dir = 1;
        Wind_Direction_Dir = 1;
//
// Configure TMR0 to generate interrupts every second
//
        TMR0H = 0x48;
        TMR0L = 0xD2;
        T0CON = 0x87;                       // Configure TMR0
        INTCON = 0xA0;                      // Enable TMR0 interrupts
//
// Configure Timer 1. Timer is clocked by the wind speed sensor
//
        T1CON = 0x86;
while(1)                                                    // Do forever
{
Read_Wind_Direction();
        Read_Wind_Speed();
        UART1_Write(WindDirTxt);
        UART1_Write(mphTxt);
Delay_Ms(60000);
}
}
```

Figure 8: Transmitter program

PCIM
EUROPE

International Exhibition and Conference
for Power Electronics, Intelligent Motion,
Renewable Energy and Energy Management
Nuremberg, 19 – 21 May 2015

Power for Efficiency

pcim-europe.com

More information at **+49 711 61946-0**
pcim@mesago.com or **pcim-europe.com**

mesago
Messe Frankfurt Group

PCIM EUROPE 2015
Nuremberg
19-21 May 2015
www.pcim-europe.com

PCIM
EUROPE

International Exhibition and Conference
for Power Electronics, Intelligent Motion,
Renewable Energy and Energy Management
Nuremberg, 19 – 21 May 2015

PCIM Europe 2015 – Meeting Point For Experts From Industry And Science

From 19-21 May 2015 many international companies will present their latest products, research findings and innovations in the field of power electronics at PCIM Europe in Nuremberg. Around 400 exhibitors will demonstrate their recent developments, offering a unique sector overview to more than 8000 visitors.

Power Electronics Conference

In parallel with the PCIM exhibition, the conference will feature 29 presentations and poster sessions, giving a thorough overview of trends and developments in the industry. Among the highlights of this year's conference are three top-class keynotes on "*The State of the Art and Future Trends of Power Semiconductor Devices*", "*Packaging and Reliability of Power Modules – Principles, Achievements and Future Challenges*" and "*Electrochemical Battery Management and Applications*".

In addition, on the two days before the conference, 17-18 May, there will be nine seminars and nine tutorials, where renowned industry experts discuss their views of the industry. At the Industry Forum in Hall 6, there will be more technical presentations, expert discussions, project presentations and market overviews from associations, specialist media and companies.

The exhibitor forum in Hall 7 will offer another 50 presentations, focusing of the latest developments and innovations from the exhibiting companies.

Free Entry

The event is free, but registration is required. Learn more at **www.pcim-europe.com/tickets**

Telecoms iQ
a division of IQPC

Network with Wearable experts and enter the discussion on the future of Wearables

27th – 28th May, 2015 | London, UK

WEARABLES Europe

Shaping the future of Wearable Technology and driving consumer adoption for this new market

Featuring experts from across the wearable technology market including:

Sonny Vu,
CEO & Founder,
Misfit Wearables

Grant Allen,
Technology Program Manager & Principal Architect,
Google

Michael Apollo,
Head of Mind Sciences,
Interaxon

Amish Patel,
Head of Experiences and Design,
Microsoft Band

Barry McNeill,
CEO of Europe, ME & Asia,
Catapult Sports

Dan Cui,
Vice President Sales & Business Development,
Vuzix

Michael Dillhyon,
President,
Vital Connect Europe

Pierre-Yves Frouin,
CEO,
Bioserenity

Take advantage of leading case studies:

- **Novelty Vs Authenticity** – Discover how a device with high levels of authenticity will result in continuous engagement and persistent use by customers with Catapult
- **Wearables in Enterprise** – Explore the unique ability of wearable devices to improve enterprise efficiency and safety
- **Medically Accepted Wearable Device** – Hear from Vital Connect Europe and discover how they have created a medically accepted and regulated wearable device
- **Consumer Adoption** – Discover methods to increase consumer adoption for your device in this fragmented marketplace
- **Wearable Business Models** – Develop a business model specific to your wearable device and differentiate yourself in this crowded ecosystem
- **Quantified Self to Functional Self** - A case study from Interaxon exploring the importance of analysing your data to provide functional information and meaningful insights

Find out more @ **www.wearables-europe.com/agenda**
Get involved on twitter **#WearablesEurope**

OLSON®

UK's No.1 IEC Connection

CALL OUR SALES HOTLINE

020 8905 7273

VISA MasterCard Maestro

24 HOUR DELIVERY SERVICE

ISO 9001 REGISTERED FIRM GB 1907

OLSON ELECTRONICS LIMITED
OLSON HOUSE, 490 HONEYPOT LANE, STANMORE, MIDDX HA7 1JX
TEL: 020 8905 7273 FAX: 020 8952 1232
e-mail: sales@olson.co.uk web site: http://www.olson.co.uk

WÜRTH ELEKTRONIK EISOS OFFERS SMD AIR COILS FOR HIGH-FREQUENCY APPLICATIONS

High-frequency applications, especially in the area of radio technology, require air coils with a particularly high Q-factor. Specifically adapted to the current market requirements for such applications, Würth Elektronik eiSos is now expanding its portfolio of WE-CAIR air coils with new design types 1322 and 1340.

The new coils are one-third flatter than the current generation in the series. The new 1320 type has a 20% higher rated current with the conventional ceramic coils in the 0805 chip format. Its high Q-factor remains stable even in the high MHz range, enabling these extremely flat air coils to be used over a broad spectrum of frequencies.

Thanks to the air coil, the inductance can be kept constant all the way into the GHz range.

Samples are available free of charge on request. All products are available from stock.

www.we-online.de

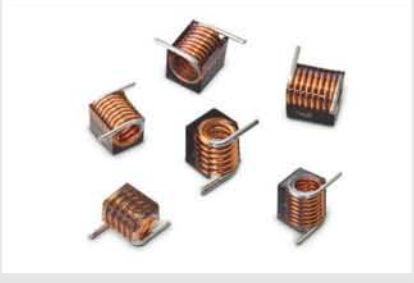

NEW MULTI-PIXEL GAS SENSOR AND NEW BAROMETRIC PRESSURE SENSOR FROM SENSIRION

At the 2015 Mobile World Congress in Barcelona, Sensirion presented a new multi-pixel gas sensor and a new barometric pressure sensor. Both sensors, which rank among the smallest yet most accurate in their class, are capable of measuring indoor air quality (IAQ), the gases in a person's breath, and barometric air pressure, as required for indoor navigation applications. The new sensors complement Sensirion's existing product offering for wearables, smartphones, tablets and the Internet of Things (IoT), and confirm the company's status as the only sensor manufacturer to offer a complete solution all the way from sensor to cloud.

With its trusted humidity and temperature sensors already established on the market, Sensirion is now expanding its range of environmental sensors to include gas and pressure sensors.

www.sensirion.com

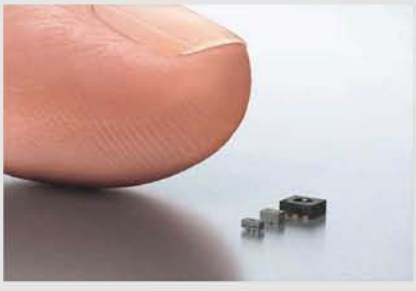

NEW HIGH-POWER WR28 WAVEGUIDE DUAL-CHANNEL ROTARY JOINT

The New AM28RJD dual-channel rotary joint from Link Microtek provides an effective means of reducing component count and saving space and weight in the compact antennas that are used for Ka-band high-data-rate SOTM (satellite-on-the-move) communication systems.

Particularly suitable for military or commercial airborne systems such as satcom uplinks in unmanned aerial vehicles, the new rotary joint features a high-power/low-loss WR28 waveguide transmit channel, together with a coaxial receive channel offering a high current rating of 2A at 24VDC, which enables it to power the antenna's LNB and servo motors without the need for additional slip rings.

The central transmit channel has a frequency range of 29-31GHz, with an average power rating in excess of 50W, a typical insertion loss of just 0.5dB and a maximum VSWR of 1.7:1.

www.linkmicrotekeng.com

TEKTRONIX ANNOUNCES 70GHZ REAL-TIME OSCILLOSCOPE

Tektronix announced the DPO70000SX 70GHz ATI (Asynchronous Time Interleaving) performance oscilloscope featuring one of the lowest noise and highest effective bits of any ultra-high bandwidth real-time oscilloscope around. The new oscilloscope incorporates a range of innovations that enable it to more effectively meet the current and future needs of developing high-speed coherent optical systems or performing leading-edge research.

Additional key innovations in the DPO70000SX ATI include 200GS/s sample rate with 5ps/sample resolution for improved resolution and timing; compact form-factor that enables the instrument to be positioned very close to the device under test (DUT); scalability; precise data synchronization and convenient operation of multi-unit systems.

Through the use of ATI technology, DPO70000SX oscilloscope enables engineers to see more of their signal details with less noise and distortion for better measurements and system operation.

www.tektronix.com

SPEEDBOARD ASSEMBLY SERVICES INVESTS IN SELECTIVE SOLDERING

UK based contract electronics manufacturer Speedboard Assembly Services has invested in an ERSA Versaflow 345 in-line selective soldering system, enabling to tackle increasingly complex double-sided, mixed-technology PCB assembly projects, and in particular boards that must be manufactured to the IPC-A-610 Class 3 standard.

Whilst some double-sided, mixed-technology PCBs can be manufactured using wave soldering – using either a glue and wave process or pallets to mask underside SMDs – this is becoming increasingly impractical for densely populated boards.

Selective soldering has much in common with wave soldering – in terms of fluxing, pre-heating and soldering stages – but components are soldered on a pin-by-pin basis and without disturbing pre-placed neighbouring components.

www.speedboard.co.uk

LOW-LOSS AND PRECISE CHIP FUSES FROM SCHURTER

Schurter chip fuses are available in a number of different current ratings from 50mA to 25A at a rated voltage of up to 125VAC/VDC. Depending on the version and voltage ratings, a breaking capacity of up to 600A is reached. Thanks to these impressively high values and variety, the Schurter chip fuses can be used in a wide range of applications; they are especially suitable for mobile and battery-operated devices, in sensor technology and industrial electronics.

Schurter chip fuses set themselves apart from comparable products through their extremely precise opening times and minimal power dissipation. In addition, their solid construction makes them especially resistant to vibrations and pulse loads. Furthermore, the SMD contacts, some of which are gold-plated, have a positive influence on the wettability, storage life and electrical quality of the chip fuses.

www.schurter.co.uk

NEW, HIGH RIPPLE-CURRENT HYBRID CAPACITORS FROM PANASONIC

Panasonic Automotive and Industrial Systems has introduced a new series of conductive polymer hybrid aluminium electrolytic capacitors with 45% higher ripple current, suitable for high reliability applications that require low leakage, high capacitance and high stability.

The 125°C hybrid capacitors in 25V and 35V now feature a ripple current of up to 2900mA$_{rms}$. This is the best performance available for such small devices and approaches the ripple current performance of solid polymer devices (10.2mm maximum height) but with the many advantages of the hybrid polymer capacitor technology including low power consumption and the ability to withstand test environmental conditions (85degC/85%/2000 hour RH).

Capacitance values are 10-330µF; the devices can withstand voltages of 25-63V, and endurance is 4000 hours at 125degC.

http://eu.industrial.panasonic.com/

SURFACE-MOUNT PRODUCTS FOR EFFECTIVE EMI/RFI SOLUTIONS

Harwin has announced a package of surface mount products that can be used separately or in combination to deliver an effective EMI/RFI solution. All the products – part of the Harwin's EZ-BoardWare range – are designed to take advantage of surface mount technology, simplifying and accelerating manufacture, reducing costs and increasing quality.

EZ-BoardWare shield cans are simply pressed onto pre-positioned surface mount EZ-Shield clips, forming a Faraday cage around sensitive ICs and electronic circuitry, which will help save expensive, labour-intensive secondary assembly and facilitates rework.

A range of can sizes and clips are available. Attenuation performance up to 24dB can be achieved, depending on frequency and configuration. The cans have a simple, five-sided box design, which is mechanically robust and more cost-effective than fence and cover types.

www.harwin.co.uk

NEW ICE40 ULTRALITE DEVICE ACCELERATES TIME TO MARKET

Lattice Semiconductor has added a new iCE40 UltraLite FPGA, aimed at enabling manufacturers accelerate time to market of mobile devices with unique and compelling features. This newest FPGA is one of the most compact and lowest power device around. Its features will enable manufacturers to add easily multiple capabilities to their mobile devices including TV remote control thanks to its IR control and learning mode capability, RGB LED control to simulate multi-color effects for notification, white LED control to enable flashlight functions on smartphones, motion gesture that reduces the need to use the touch screen to awaken devices and launch applications, high accuracy pedometer that requires very little power, and maximized battery life among others.

www.latticesemi.com

OMC EXPANDS UK MANUFACTURING FACILITY

OMC is expanding its UK manufacturing facility in Cornwall to double the current floor space and increase production capacity. Work has already started on a brand new factory at the company's Redruth site.

"The decision to expand our capacity further has been driven by demand for our fibre optic transceivers and cable assemblies," said William Heath, OMC's Commercial Director. "We are seeing increased demand from industry as firms integrate Smart Factory/Industry 4.0 related facilities into their designs, which require large amounts of equipment performance data to be collected in order to fine-tune production processes, increase output and give companies a competitive edge."

The new factory is expected to be operation in mid to late summer of this year.

www.omc-uk.com

1200V/1700V SCALE-2+ DUAL-DRIVER-CORE FAMILY EXTENDED

Power Integrations launched its latest SCALE-2+ dual IGBT-driver core, the 2SC0435T2G1-17, the most compact product in its power range with a footprint of only 57.2 x 51.6mm and a height of just 20mm. The new SCALE-2+ technology enables Soft Shut Down (SSD) to be implemented in the event of a short circuit without requiring additional components. This is particularly beneficial in applications with low stray-inductance where full Advanced Active Clamping (AAC) may not be required. If desired, the core can also provide full AAC.

Designed to drive all standard 1200V and 1700V IGBTs, the 2SC0435T2G1-17 driver core features an embedded paralleling capability to simplify inverter design at high power ratings. Multi-level topologies are also supported.

www.power.com

AWS INTRODUCES REAL-TIME OPERATIONAL CONTROL SYSTEM

AWS, a specialist contract electronics manufacturer, has announced that it has developed and implemented an updated real-time control system at its manufacturing plants in the UK (Newcastle-under-Lyme) and Slovakia (Namestovo) to cover every aspect of its business at the two facilities. The £50,000 bespoke ERP system enables the company to monitor activities and provide immediate feedback to customers concerning their orders.

"We have been working on our vision for full shopfloor control to supplement our current system for some time and we are now ready to enter the era of the Smart Factory – or Industry 4.0. We measure our manufacturing performance in real time, at all process stages and on all machines through real time scanning and operator sign off," said AWS CEO, Paul Deehan.

www.awselectronicsgroup.com

PULSONIX ANNOUNCES THE APPOINTMENT OF 3D TRONIC

Westdev Ltd, the PCB EDA company, announced it had signed 3D Tronic to sell and support Pulsonix in Brazil. 3D Tronic boasts a wealth of experience in the EDA industry.

Introduced in 2001, Pulsonix EDA software has set the standard for high-performance schematic design capture, simulation, PCB layout and autorouting. Developed by a dedicated in-house team, each release introduces new key features, offering users flexible and highly compatible software that meets the demands of PCB design today.

3D Tronic was founded to support the Brazilian electronics industry by providing EDA solutions and new technologies such as 3D-MID (Molded Interconnect Device). The 3D Tronic offers training, technical support and services to its customers.

www.pulsonix.com

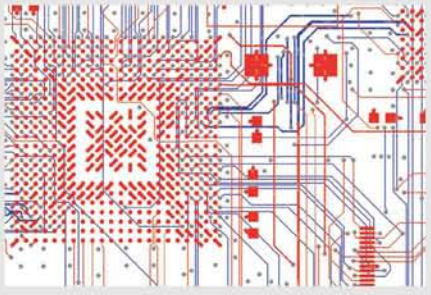

TELEDYNE LECROY ANNOUNCES FIRST MOTOR DRIVE ANALYZER

Teledyne LeCroy launched the MDA800 Series of Motor Drive Analyzers (MDAs) that combine three-phase power analyzer static (steady-state) calculations, unique dynamic three-phase power and mechanical motor analysis capabilities, and high bandwidth (1GHz) embedded control system debug in a single instrument.

The MDAs are based on the HDO8000 oscilloscope platform and are standard with 8 input channels (and optional 16 digital channels) with 12-bit resolution, 2.5GS/s sample rate, up to 1GHz bandwidth and up to 250Mpts/ch acquisition memory. A complete set of serial trigger/decode and analysis software options, and a wide variety of voltage and current probes are available to use with the MDAs.

Design engineers that integrate motors into their designs (vehicles, power tools, appliances, elevators, fans, blowers, compressors, pumps, etc.) will use this product to validate proprietary controls and complete drive system designs.

www.teledynelecroy.com

60V/4A & 36V/8A BUCK-BOOST MODULE REGULATORS

Linear Technology has introduced a new family of buck-boost µModule (micromodule) regulators. The LTM8055 and LTM8056 seamlessly regulate an output voltage equal to, greater or less than the input voltage. Housed in a 15 x 15 x 4.92mm BGA package, these devices include the inductor, DC/DC regulator, MOSFETs and the supporting components.

The LTM8055 operates from input voltages ranging from 5V to 36V, delivering a load current up to 8A. The LTM8056 has a higher input voltage, up to 60V with 4A load current capability. The compact solution provided by these devices free PCB board space in systems such as battery operated devices, industrial control, avionics and solar-powered equipment.

For battery charging or precision load current adjustment, both devices enable input and output average current limit setting.

www.linear.com

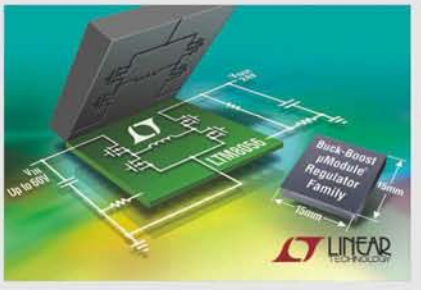

HALL-EFFECT SPEED/DIRECTION SENSOR IC WITH HYSTERESIS DETECTION

The new A1232 from Allegro MicroSystems Europe is a Hall-effect speed and direction sensor IC with built-in hysteresis detection. This is a highly sensitive temperature-stable magnetic sensing device, ideal for use in ring magnet based speed and direction sensing systems in harsh automotive and industrial environments. It is the first device of its kind with the ability to detect when it powers up in the magnetic hysteresis band, reducing angle accuracy error that occur when edges are missed at start-up.

The Allegro A1232 includes dual Hall elements spaced 1.63mm apart that are photolithographically aligned to within 1µm. The precise spacing of the sensing elements eliminates a major manufacturing hurdle encountered when using fine-pitch ring magnets. The signals from the dual Hall elements are encoded into logic outputs representing the speed and direction of the target.

www.allegromicro.com

NEW CODESONAR RELEASE FOR THE IoT ERA

GrammaTech introduced CodeSonar 4.1, the latest version of the company's software analysis tool for C/C++, Java and binaries. The latest version of CodeSonar includes new distributed analysis capabilities, deeper tainted data analysis and binary analysis support for x64 processors. Combined, these advances will help developers build more stable and secure code in the Internet of Things (IoT) era, where a growing number of embedded software systems are networked enabled in sometimes unpredictable and often unsecure ways.

CodeSonar is ideal for zero-defect tolerance embedded environments because it analyzes both source and binary code to identify serious security and quality liabilities that cause system crashes, memory corruption, data races and other unexpected vulnerabilities.

As the pressures and liabilities of software supply chain management (SSCM) continue to increase, embedded teams must investigate both source code and binaries to ensure consumer safety.

www.grammatech.com

RUTRONIK EXHIBITS COMPLETE SOLUTIONS AT PCIM

Rutronik Elektronische Bauelemente will exhibit a range of power semiconductor innovations from leading manufacturers at PCIM next month, at booth 226 in hall 7. Together with components from the passive and electromechanical sectors, they enable energy-efficient solutions and effective heat management.

For motor control, traction and drive technology in railway and utility vehicles as well as agricultural machines, inverters and renewable energies, Rutronik will show an extensive portfolio of power semiconductors, passive and electromechanical components.

The Industrial Power Control (IPC) portfolio from Infineon is a particular highlight at the Rutronik booth. It spans IGBTs as discrete products and modules, modular and disk thyristors and diodes, and driver ICs and boards for applications in power categories from 0.5kW right up to several MW.

A further focus will be on SiC components such as SiC-MOSFETs, SiC power modules and SiC diodes.

www.rutronik.com

Software Defined Magnetic Sensor

World's First Software-Defined Magnetic Sensor

Melexis introduces a new, fully programmable, extremely compact sensor IC for accurately measuring magnetic flux in X, Y and Z axes. Employing patented Triaxis® technology, the MLX90393 enables flexible Software Defined Solutions for:

- Joystick
- Slide switches
- Push/Pull Switches
- Levelers
- Linear slide switches and pots
- Rotary Knobs
- Complex 3D position sensing systems.

Micro Power and Micro Size

Suitable for micropower applications, the MLX90393 draws just 2.5µA of current when idle and features a "wake-up" on magnetic state change feature for intelligent magnetic sensor system behavior. Supporting an operational temperature range of -40°C to +85°C, the MLX90393 is supplied in a ultra small 3mm x 3mm QFN package.

Kickstart YOUR Software Defined Sensor NOW! EVB's and Example Code Available At:

www.melexis.com/MLX90393

We Engineer
The Sustainable Future.

Melexis
Microelectronic Integrated Systems

uk.mouser.com

The Newest Products for Your Newest Designs®

The **widest selection** of the **newest products**.

Over **4 million** products from over **500 manufacturers.**

Authorised distributor of semiconductors
and electronic components for design engineers.

MOUSER ELECTRONICS.